Scholars' Mine

Doctoral Dissertations   Student Theses and Dissertations

Fall 2007

Incipient continental rifting: insights from the Okavango Rift Zone, northwestern Botswana

Baraka D. Kinabo

Follow this and additional works at: https://scholarsmine.mst.edu/doctoral_dissertations

Part of the Geology Commons, and the Geophysics and Seismology Commons

Department: Geosciences and Geological and Petroleum Engineering

Recommended Citation

INCIPIENT CONTINENTAL RIFTING: INSIGHTS FROM THE OKAVANGO

RIFT ZONE, NORTHWESTERN BOTSWANA

by

BARAKA DAMAS KINABO

A DISSERTATION

Presented to the Faculty of the Graduate School of the

UNIVERSITY OF MISSOURI-ROLLA

In partial Fulfillment of the Requirements for the Degree

DOCTOR OF PHILOSOPHY

in

GEOLOGY and GEOPHYSICS

2007

ESTELLA A. ATEKWANA, advisor	**JOHN P. HOGAN, co advisor**
DAMIEN DELVAUX	**MOHAMED ABDELSALAM**
	STEPHEN GAO

PUBLICATION DISSERTATION OPTION

This dissertation is organized into two sections and two journal articles. Section one gives an outline of the dissertation and introduces the problem, tectonic framework, objectives, available data and research plan. The first article "Early structural development of the Okavango Rift Zone, NW Botswana", from page 14 to 49, has been published in the *Journal of African Earth Sciences, volume 48, page 125-136.* The second paper "Fault growth and propagation during incipient continental rifting: Insights from a combined aeromagnetic and SRTM DEM investigation of the Okavango Rift Zone, NW Botswana", from page 49 to 91 has been submitted to *Tectonics* and is in the second round of review. Section two summarizes the major conclusions and includes recommendations for future work.

ABSTRACT

In this dissertation aeromagnetic, gravity, and Shuttle Radar Topography Mission Digital Elevation Model (SRTM DEM) data from the Okavango Rift Zone in northwest Botswana are used to map the distribution of rift and basement structures. The distribution of these structures provide useful insights into the early stages of continental rifting. The objectives of this study are (1) assessing the role of pre-existing structures on rift basin development, (2) characterizing the geometry of the nascent rift basins, (3) documenting fault growth and propagation patterns, and (4) investigating the border fault development. Potential field data especially aeromagnetic data are used to map out structures in the sediment covered basement, whereas SRTM DEM data express the surface morphology of the structures. The azimuth of rift faults parallel the orientation of the fold axes and the prominent foliation directions of the basement rocks. This indicates that pre-existing structures in the basement influenced the development of the rift structures. NE dipping faults consistently exhibit greater displacements than SE dipping faults, suggesting a developing half-graben geometry. Individual faults grow by along axis linkage of small segments that develop from soft linkage (under lapping to overlapping segments) to hard linkage (hooking, fused segments). Major rifts faults are also linking through transfer zones by the process of "fault piracy" to establish an immature border fault system. The relationships between scarp heights and vertical throws reveal that the young and active faults are located outside the rift while the faults with no recent activities are in the middle suggesting that the rift is also growing in width. This study demonstrates the utility of potential field data and SRTM DEM to provide a 3-D view of incipient continental rifting processes such as fault growth and propagation.

ACKNOWLEDGMENT

TABLE OF CONTENTS

PAPER

LIST OF ILLUSTRATIONS

PAPER 2: FAULT GROWTH AND PROPAGATION DURING INCIPIENT
CONTINENTAL RIFTING: INSIGHTS FROM A COMBINED
AEROMAGNETIC AND SRTM DEM INVESTIGATION OF THE
OKAVANGO RIFT ZONE, NW BOTSWANA

LIST OF TABLES

1. INTRODUCTION

1.1. DISSERTATION OUTLINE

Section one gives an overview of the problem statement and research objectives. A general introduction to the study area including the tectonic setting of the entire East African Rift System, the Southwestern Branch, and the Okavango Rift Zone (ORZ), is also given. Available data sets used in this study are also mentioned.

The two peer reviewed journal papers discuss the four main objectives of my research as follows. **Paper one** (**Kinabo et al., 2007**) discusses objectives 1 and 2 of this study which are assessing the role of pre-existing structures in rift development and characterizing the early geometry of the rift basin, respectively. The results reported in this paper suggest a strong influence of pre-existing basement fabric on the development of the rift. Gravity models suggest that the geometry of the Okavango Rift Zone is transitional from a synformal basin to a half-graben consistent with the presence of an immature border fault system along the southeastern side of the rift. **Paper two** (**Kinabo et al.,** *in review*) discusses objectives 3 and 4, which are documenting the fault growth and propagation patterns and investigation the border fault development respectively. The results suggest that individual rift faults grow from along axis linkage of small faults, which in turn link along transfer zones to form a developing border fault system for the ORZ. The results also suggest that the rift is growth both in width and length.

Section two presents the dissertation's major conclusions, which represent the outcomes and contribution of this research. The section also offers recommendations for future work based upon the questions that have been raised in this dissertation.

1.2. PROBLEM STATEMENT

Previous studies of active rift basins worldwide have focussed on the correlation between pre- and syn-rift structures to determine the role of inherited structures on rift development (e.g., Rosendahl, 1987; Ebinger, 1989; Ring et al., 1992; Morley, 1999). However, little is known of the actual initial development of fault systems bounding rift basins and how they link to form discrete basins and subsequently rift systems. Important unanswered questions regarding the initiation and development of continental rifts are (1) how do border fault systems bounding rift basins evolve? Do they grow from the linkage of several small faults, or the along-axis propagation of one fault? (e.g., Cowie, 1998). It has been obvious to geologists that larger faults grow by linkage of small faults. However, the timing of border faults development relative to the associated basins and the evolution of small faults into border faults are still controversial questions. Morley (2002) recognizes three models for early fault linkage, as follows (a) linkage prior to significant basin formation, (b) linkage after basin formation (e.g. Usangu flats, Tanzania), and (c) linkage during basin development (e.g. Lokichar, Kenya and Lupa fault, Tanzania); (2) how valid are models for the border fault development when tested against natural examples? and (3) to what extent do pre-existing structures influence the development of nascent rifts? It is now obvious to scientists (e.g., Morley, 1999; Davis and Reynolds; 1996) that if the pre-existing structures are oriented in the direction that intersects the sliding friction failure envelope, they will be reactivated by later events of deformation. However, the extent to which pre-existing structures influence fault development in young rifts is still a topic of considerable interest. Within the more

evolved northern part of the East African Rift System (EARS) and other rifts (e.g. Baikal Rift in Siberia, Rio Grande Rift in North America) border faults are already fully developed, therefore only a few natural examples of young rifts exist that permit us to address the above questions regarding border faults development and their relationship to the bounding basins. Nascent rifts (e.g., the Okavango Rift Zone; ORZ) provide a unique opportunity to study the early stages of continental extension, prior to the accumulation of significant amounts of sediments, volcanism, and multiphase deformation that often obscure the investigation of these early time processes in more evolved continental rift zones. This study integrates high resolution potential field (aeromagnetic and gravity), remote sensing, and outcrop data from the ORZ to address the following objectives: (1) assessing the role of pre-existing structures on rift basin development, (2) characterizing the geometry of the rift basins, (3) documenting fault growth and propagation patterns, and (4) investigating the border fault development. The results of this study should therefore broaden our understanding of fault growth and shed more light on the development of border and transfer faults in developing continental rifts.

1.3. THE EAST AFRICAN RIFT SYSTEM

The East African Rift System (EARS) is a classic example of continental rifting (Chorowicz, 2005 and references therein). The rift valley is a topographic manifestation of extensional tectonic processes that are working to pull apart the African continent. A unique characteristic of the EARS is that it includes all stages of continental rifting from nascent rifting (in the Okavango Rift Zone), rift to drift (in the northern Main Ethiopian Rift and the Afar) to sea floor spreading (in the Red Sea and Gulf of Aden; Fig. 1.1).

Traditionally, this rift system is divided into the Eastern and Western branches

(Fig. 1.1). The 25 to <1 Ma Eastern Branch extends from the Afar Depression in Ethiopia in the north through the Kenya and Turkana rifts in Kenya to central Tanzania in the south. The initial rifting process in Afar started in Miocene and intensified in Pliocene (Morley et al., 1999). The younger (<15 Ma) and less evolved Western Branch mimics the western boundary of the mechanically strong and cold Tanzania Archaean Craton and extends from Lake Albert in Uganda in the north and into western Tanzania (i.e., Lake Tanganyika, Lake Rukwa), to Malawi (Lake Nyasa/Malawi) and Dombe in Mozambique (Kampunzu et al., 1998; Ebinger, 2004). Generally, both the Eastern and Western rifts are segmented along their lengths into a series of asymmetric basins bounded by en echelon curvilinear border faults. Volcanism is widespread in the Eastern Branch and rare in the Western Branch. The individual rift basins (50-100 km long and 40-100 km wide) are linked by transfer faults/accommodation zones (Rosendahl, 1987; Ebinger, 1989) and typically filled by substantial amount of sediments including fluvio-deltaic and lacustrine sediments and/or volcanics and volcanoclastics.

Recent lithospheric studies such as the Ethiopia Afar Geoscientific Lithospheric Experiment (EAGLE) in the EARS suggest that the upper crust within the rift is characterized by higher than usual seismic velocities (~5-10 %) due to magmatic under-plating whereas the upper mantle velocities are reduced by 2-4% due to the presence of partial melts (Maguire et al., 2003; Mackenzie et al., 2005; Bastow et al., 2005). Representative continental rifting evolutionally models from the EARS reveal the relative importance of border faults and magma up-welling as rifting proceeds to seafloor spreading (Fig. 1.2). These models suggest that asthenospheric processes (in the form of mantle upwellings) dominate over lithospheric processes (in the form of movements

along the detachment faults) during the rift-drift stage (Keranen et al., 2004; Ebinger and

Casey, 2001; Ebinger, 2004).
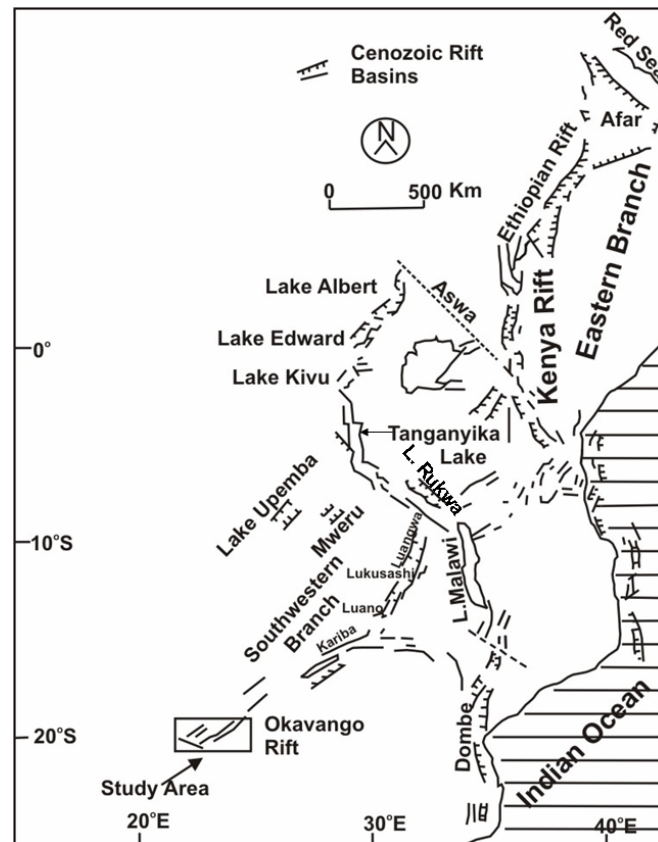
Figure 1.1: Map of the East African Rift System (EARS) showing the location of the

Southwestern Branch (modified from Kampunzu et al., 1998).
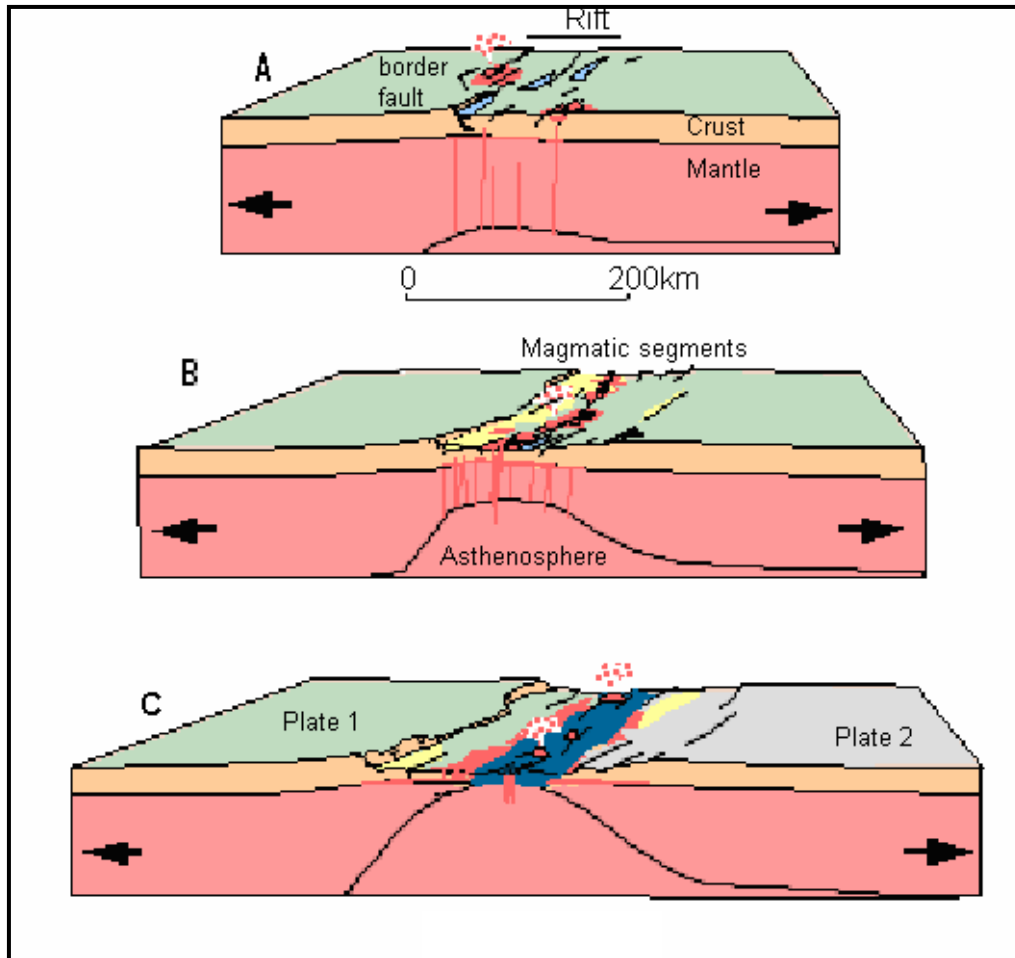
Figure 1.2: Models of continental rift evolution from the EARS showing the relative strain accommodation as rifting proceeds to seafloor spreading: (a) Initial continental rifting stage, most of the strain and magmatism are restricted to the border faults; (b) transitional rifting stage, strain is accommodated by both border faults and magmatism, example of this stage is the central Eastern Rift (Kenya Rift); and (c) immediately before continental breakup, at this stage most of the strain (up to >50%) is accommodated by the magmatism at the center of the basin and the border faults are abandoned, an example of this stage is the northern Main Ethiopian Rift. Reproduced from Ebinger, 2005

1.3.1. The Southwestern Branch. Some authors have suggested an extension of the EARS into Zambia, southeast Congo, and Botswana, forming a Southwestern branch (e.g. Fairhead and Girdler, 1969; Reeves, 1972; Chapman and Pollack, 1977; Ballard et al., 1987; Sebaganzi et al., 1993; Girdler, 1975; Modisi et al., 2000; Sebagenzi and Kaputo, 2002). The Southwestern branch consists of a network of separate Quaternary rift basins distributed along an approximately 250 km wide corridor extending for about 1,700 km west of Lake Tanganyika with the ORZ at its southern tip (Fig.1.1). The rift basins have an average length of 100 km and widths of 40-80 km (Modisi et al., 2000). The basins of the Southwestern branch include; Luangwa, Luano, Mweru and Lukusashi (in Zambia), Upemba (in Democratic Republic of Congo), and Okavango (in NW Botswana). Sebagenzi et al. (1993) indicate that the Southwestern branch is characterized by regional gravity anomalies of -106 to -140 mGal and heat flow values in the range of 53-76 mW/m^2 suggesting that the regional gravity anomaly may be explained by the upwelling of low density asthenosphere and thin lithosphere (123 km) associated with rifting. Prior to this dissertation this branch has received little attention since it was first discovered about three decades ago. Thus our understanding of its development and relationship to the more evolved branches of EARS is limited and unclear.

1.3.2. The Okavango Rift Zone. Geological and geophysical investigations of the ORZ are sparse. Fairhead and Girdler 1969 were probably the first scientists to recognize the existence of the rift in the southern Africa including the area that is now known as the Okavango Rift Zone. Later, Scholz et al. (1976) studied earthquake data from the ORZ and determined that the rift faults in this basin are active. More recently, Modisi et al. (2000) used high resolution aeromagnetic data to study fault kinematic of the ORZ. The major findings of their work are that (1) the width of this rift is similar to that of the more mature basins of the EARS, and (2) preexisting structures exert a major control over the rift development. However, limited aeromagnetic data from the southern part of the rift were available at the time of their study preventing proper delineation of the full extent of the rift structures. Recent availability of extensive data such as magnetic, gravity, and SRTM DEM, covering the entire ORZ provides an opportunity to map out the full extent of the faults and investigate the initiation of a continental rift in greater detail.

The following is a summary of tectonic framework of the ORZ, based upon the results of my investigations and is described in greater detail in papers, one and two. The ORZ, in NW Botswana is located at the southernmost tip of the EARS (Fig. 1.1). It consists of three developing depocenters defining developing half-grabens, namely from south to north, the Ngami, Mababe, and Linyanti-Chobe (Fig. 1.3). The ORZ is characterized by 10 northeasterly trending faults including the Thamalakane, Kunyere, Linyanti, Chobe, Nare, Phuti, Lecha, Tsau, Gumare and Mababe (Fig. 1.3). These faults define a northeast trending rift zone that is ~400 km long and ~150 km wide. Several faults including Gumare, Kunyere, Chobe, Thamalakane, Phuti, Mababe, and Linyanti

have scarps that can be recognized on the SRTM DEM. The faults' vertical throw range is ~17-334 and scarp elevations range from ~2-44 km.

Rift faults are propagating by along axis linkage of small segments which are 3-15 km long to from major rift faults that are 25-325 km long. The linkages can be characterized as soft linkage (e.g., linkage along the Thamalakane Fault) or hard linkage (e.g., linkage along the Mababe, and Gumare faults). The rift lacks a well developed border fault and its geometric shape can be best described as transitional between a synformal basin and a developing half-graben consistent with an early rift stage. Additionally, the major rift faults are also linking along transfer zones through a process of "fault piracy" as in the case of the Thamalakane and Phuti linking into the Mababe in the north near the Mababe Graben and the Thamalakane with the Kunyere faults in the south near the Ngami Graben to define a developing immature border fault. Faults' throw and elevation scarp heights suggest that the rift basin is also widening. Pre-existing basement structures exert a profound influence on the initiation and development of the rift faults and linkages.
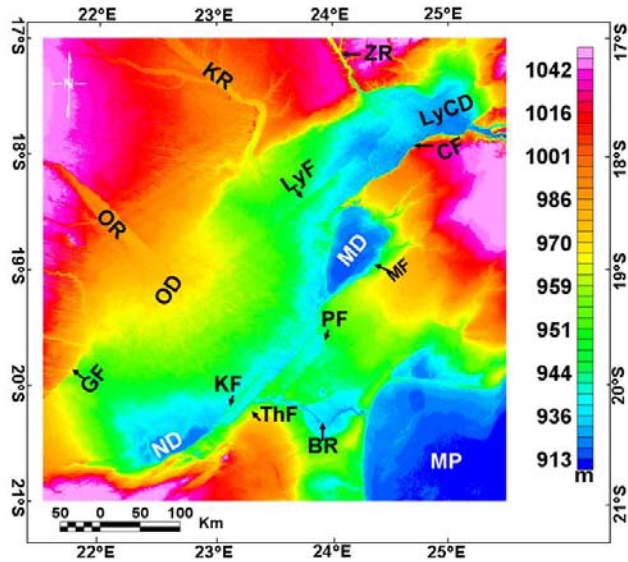
Figure 1.3: SRTM DEM map of the Okavango Rift Zone showing major rift faults and depocenters. GF = Gumare Fault, KF = Kunyere Fault, ThF = Thamalakane Fault, PF = Phuti Fault, MF = Mababe Fault, CF = Chobe Fault, LyF = Linyanti Fault, MP = Makgadikgadi Pans, ND = Ngami Depression, LyCD = Linyanti- Chobe Depression, and MD = Mababe Depocenter.

1.4. AVAILABLE DATA

Datasets available for this project include: (1) Shuttle Radar Topography Mission-Digital Elevation Model (SRTM DEM), (2) field outcrop data, and (3) high resolution aeromagnetic (250 m line spacing), and gravity (7.5 km grid) data.

Shuttle Radar Topography Mission-Digital Elevation Model data are distributed by the National Aeronautical and Space Administration, Jet Propulsion Lab in 1°x1^{o} tiles with DEM already extracted. The data are available online and can be downloaded free of charge from the National Aeronautical and Space Administration (NASA) website

(ftp://e0mss21u.ecs.nasa.gov/srtm). Two types of SRTM data are available: one arc data (SRTM-1, 30 m resolution); and three arc data (SRTM-3, 90 m resolution). SRTM-3 (DEM) data are used in this study.

Aeromagnetic data were acquired in 1996 by the Geological Survey of Botswana. The flight elevation for the aeromagnetic data was 80 m along north-south lines with 250 m east-west line spacing and tie lines were spaced 1.25 km apart. The Geological Survey of Botswana also acquired gravity data in 1999. The survey was helicopter aided with an acquisition accuracy of 0.2 mGal on a 7.5 x 7.5 km grid.

1.5. RESEARCH PLAN

This research addresses the following four goals: (1) assessing the role of pre-existing structures on rift basin development, (2) characterizing the geometry of the nascent rift basins, (3) documenting fault growth and propagation patterns, and (4) investigating the border fault development. The objectives are described in more details below.

1.5.1. Objective 1 − Influence of Pre-existing Structures. In objective 1, I examine the influence of basement fabric in rift development. To archive this goal, I use aeromagnetic data from the ORZ. An orthogonal relationship between the rift faults and the Karoo dikes exists (Modisi et al, 2000). This relationship allows the faults to be recognized when examining the dikes they displace. I apply vertical derivative filters in order to enhance shallow features corresponding to the geology and filter the effects of the deep seated features. Vertical derivative maps provide an excellent picture of rift faults in the ORZ. Azimuths of the dominant rift and basement structural features were measured from the vertical derivative maps. The influence of pre-existing structures on

the rift development was examined by comparing the azimuths of rift faults with those of the basement structures on Rose diagrams. Coincidence or mismatch of these orientations will be used as a measure of how much the pre-existing fabric has influenced the rift.

1.5.2. Objective 2 – Geometry of Rift Basins. Construction of the shape of the rift basin requires that throws and dip direction of the faults to be known. Because only limited borehole data are available and because the rift is largely buried in the ORZ, potential field data are nearly the sole means for estimating the fault throws. Faults' throws were determined by calculating the differences in depths to the top of the dikes obtained from the 3-D deconvolution solutions. Dip direction of the faults were inferred from topographic profiles extracted from SRTM DEM.

I have also prepared 2 ¾-D gravity forward models from the gridded data to constrain the shape of the basin and determine the thickness of its sediments. Depths obtained from 3-D Euler deconvolution solutions were used as the initial depth estimates for gravity models and the initial density values used will be estimated based on the lithologies underlying the rift basin, as discussed in Modisi et al. (2000).

1.5.3. Objective 3 - Fault Growth Patterns In objective 3, I examine the fault growth and propagation patterns in ORZ using field outcrop, potential field, and SRTM data. Integration of SRTM DEM data with high resolution aeromagnetic data will allow determination of the details of fault kinematics within the basement and at the surface. Examination of the fault scarps on the SRTM images provide information about the nature of rift fault growth and border fault development at the surface while aeromagnetic data provide information about the details of structures within the basement.

1.5.4. Objective 4 – Border Fault Development. In objective 4, I investigate a possible linkage of major rift faults on the surface and in the basement to form a major boundary fault that will accommodate most of the stress and controls the growth of the ORZ in future. I also examine the relative age and activity of the faults using determined vertical throw and scarp height to assess the growth of the rift laterally.

1. EARLY STRUCTURAL DEVELOPMENT OF THE OKAVANGO RIFT ZONE, NW BOTSWANA

B. D. Kinabo[a*], E. A. Atekwana[b], J. P. Hogan[a], M.P. Modisi[c], D. D. Wheaton[a], and A. B. Kampunzu[c].

[a]Department of Geological Sciences and Engineering, University of Missouri-Rolla, 129 McNutt Hall, Rolla, Missouri, 65409 USA

[b]Oklahoma State University, Boone Pickens School of Geology, 105 Noble Research Center, Stillwater, Oklahoma, 74078 USA

[c]Department of Geology, University of Botswana, Private Bag 0022, Gaborone, Botswana

Abstract

Aeromagnetic and gravity data collected across the Okavango Rift Zone, northwest Botswana are used to map the distribution of faults, provide insights into the two-dimensional shallow subsurface geometry of the rift, and evaluate models for basin formation as well as the role of pre-existing basement fabric on the development of this nascent continental rift. The structural fabric (fold axes and foliation) of the Proterozoic basement terrane is clearly imaged on both gravity and magnetic maps. The strikes of rift-related faults ($030\text{-}050^{o}$ in the north and $060\text{-}070^{o}$ in the south) parallel fold axes and the prominent foliation directions of the basement rocks. These pre-existing fabrics and structures represent a significant strength anisotropy that controlled the orientation of younger brittle faults within the stress regime present during initiation of this rift. Northwest dipping faults consistently exhibit greater displacements than southeast dipping faults, suggesting a developing half-graben geometry for this rift zone. However, the absence of fully developed half grabens along this rift zone suggests that the border fault system is not fully developed consistent with the infancy of rifting. Three *en échelon* northeast trending depocenters coincide with structural grabens that define the Okavango rift zone. Along the southeastern boundary of the rift, developing border faults define a 50 km wide zone of subsidence within a larger 150 km wide zone of extension forming a rift-in-rift structure. We infer from this observation that the localization of strain resulting from extension is occurring mostly along the southeastern boundary where the border fault system is being initiated, underscoring the important role of border faults in accommodating strain even during this early stage of rift development. We

conclude that incipient rift zones may provide critical insights into the development of rift basins during the earliest stages of continental rifting.

1. Introduction

Investigations of continental rifts, such as the East African rift system (EARS), have significantly improved our understanding of rifting and continental breakup (e.g., Rosendahl, 1987, Ebinger and Casey, 2001; Ebinger et al., 2004; Keranen et al., 2004). For example, in transitional continental rift environments (rift-drift stage) border faults, which control basin geometry and accommodate most of the strain during the earliest stages of rifting are   superseded by magmatic processes occurring within a narrow zone along the axis of the rift (e.g., Ebinger and Casey, 2001; Keranen et al., 2004). During this phase of rifting the lithosphere below the rifts is characterized by anomalously high heat flow and lower seismic wave velocities (e.g., Nyblade et al., 2000; Owens, 2000; Bastow et al., 2004). Such models are appropriate for processes operating during quite advanced stages of continental rift evolution. An important question remains as to what processes operate during the very early stages of continental rifting? This paper begins to address this question through a detailed gravity and magnetic investigation of the nascent Okavango Rift Zone (ORZ) in northwestern Botswana. The seismically active ORZ serves as a modern day analogue for the earliest stages of more evolved continental rift basins and provides us with a unique opportunity to investigate the early time development stage of continental rifts and address some long-standing questions related to rifting. Several authors have suggested that the structures bounding and linking rift basins are strongly controlled by pre-rift structures, implying that the along-axis segmentation of continental rifts is controlled by basement structures (e.g., Rosendahl 1987; Ring, 1994; Russell and Snelson 1994; and Morley, 1999a). However, in some cases, rift border faults appear to bear no direct correlation with the basement fabric (e.g.,

Ebinger et al., 1987). This leads to the suggestion that the development of continental rifts is controlled by deep-seated structures within the lithosphere (e.g., Delvaux et al, 1999). Thus, the role of pre-existing/inherited structures on rift development remains a long standing but important question in the study of continental rifts. In addition, very little is known about the border fault development and its relationship to basin development (e.g., Morley, 2002). Do border faults develop (a) prior to significant basin development; (b) after the basin has been established; or (c) simultaneously with the basin development? Studies of incipient rifts, such as the ORZ may shed some light on some of the above longstanding questions on continental rifting.

Although the ORZ represents an ideal location to examine the incipient stages of continental extension, previous scientific investigations have been hampered largely because the rift is mostly buried beneath sands of the Kalahari Desert. Thus, details of the structural and tectonic development of the ORZ are limited (e.g., Scholz et al., 1976; McCarthy et al., 1993; Modisi, 2000; Modisi et al., 2000; Gumbricht et al., 2001). This study has circumvented this problem by employing high resolution aeromagnetic and gravity surveys that provides an unprecedented view of the basement geology and permits us to: (1) evaluate the role of pre-existing basement fabric on the rift development, (2) map the distribution of faults and determine their displacements, and (3) provide insights into the 2-D shallow subsurface geometry and basin development of the ORZ. This information will enable us to compare the early stages of continental rifting in the ORZ with the more evolved branches of EARS to develop a more complete model for the processes involved in disaggregating continental lithosphere.
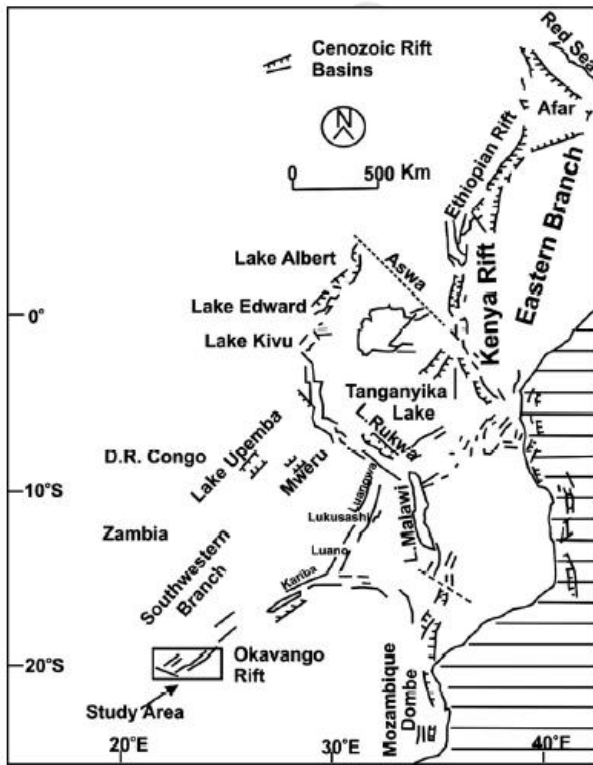
Figure 1: Map of the East African Rift System showing the location of Okavango Rift

Zone (modified from Kampunzu et al., 1998).

2. Tectonic and geologic framework

2.1. East African Rift System (EARS)

The East African rift System (EARS) is considered by many to be a classic example of a continental rift zone (e.g., Chorowicz, 2005 and references there in). Traditionally this rift system is divided in two branches, the eastern and the western branches (Fig. 1). The > 25 to <1 Ma eastern branch of the rift extends from Afar depression in Ethiopia in the north through the Kenya and Turkana rifts in Kenya, to central Tanzania in the south. The initial rifting process in Afar started in Miocene and intensified in Pliocene (Morley et al., 1999). The younger (<15 Ma) and less evolved western branch extends from Lake Albert in Uganda in the north and into western Tanzania where it is comprised by rift basins such as Lake Tanganyika, Lake Rukwa, Lake Nyasa (Malawi) and Dombe and Urema half-grabens in Mozambique (Kampunzu et al., 1998). Both the eastern and western branches are segmented along their lengths into a series of asymmetric basins bounded by en echelon curvilinear border faults and high relief. The individual rift basins are typically 50-100 km long and 40-100 km wide and filled by fluviodeltaic and lacustrine sediments and/or volcanics and volcaniclastics. Individual segments of each branch of the rift are linked together by transfer faults/accommodation zones across which reversals in basin asymmetry occur (Rosendahl, 1987; Ebinger, 1989; Chorowicz, 2005).

2.2. Southwestern branch

The EARS extends to the southwest into Zambia, southeast Congo, and Botswana where it forms a southwestern branch (e.g. Fairhead and Girdler, 1969; Reeves, 1972;

Girdler, 1975; Chapman and Pollack, 1977; Ballard et al., 1987; Sebaganzi et al., 1993; Modisi et al., 2000; Sebagenzi and Kaputo, 2002). This southwestern branch consists of a network of isolated less defined Quaternary rift basins that are distributed along an approximately 250 km wide corridor extending for about 1,700 km west of Lake Tanganyika and Lake Malawi with the Okavango Rift Zone (ORZ) at its southern terminus (Fig.1). The rift basins have an average length of 100 km in length and they are 40-80 km in width (Modisi et al., 2000). The basins include; Luangwa, Luano, Mweru, Lukusashi, in Zambia, Upemba in Democratic Republic of Congo, Kariba in Zimbabwe, and Okavango in northwest Botswana. The southwestern branch is characterized by regional gravity anomalies of -106 to -140 mGal and heat flow values in the range of 53-76 mW/m^2 (Sebagenzi et al. 1993). These authors suggest the regional gravity anomaly is best explained by upwelling of low density asthenosphere beneath a thinning lithosphere (123 km) as the result of crustal extension associated with rifting.

2.3. Okavango Rift Zone

The ORZ is developing within a large structural depression, Makgadikgadi-Okavango- Zambezi basin (MOZ) (Fig. 2) which is situated between the 1.7-3.0 Ga Congo Craton to the northwest and the 1.1-1.5 Ga Kalahari Craton to the southeast, and is superimposed on the Ghanzi-Chobe belt, a Proterozoic orogenic province. The MOZ basin is comprised of both alluvial fan deposits and deeper palaeo-lake sediments in structural depressions or sub-basins (Gumbricht et al., 2001; Ringrose et al., 2002). The MOZ basin is controlled by a series of mainly NE-SW trending faults that form grabens in the underlying basement complex and the Karoo sequence (Cooke, 1984). Tectonic activity along this trend resulted in uplift along the Zimbabwe-Kalahari axis (Thomas and

Shaw, 1991; Moore and Larkin, 2001; Ringrose et al., 2002) and displacement along northeast-southwest trending faults. This neotectonic activity resulted in the impoundment of the proto Okavango, Kwando, and upper Zambezi rivers and the development of the proto Makgadikgadi, Ngami and Mababe sub-basins (Cooke, 1984) (Fig. 2). Neotectonic activity related to the rifting in the ORZ has greatly influenced the geomorphology and drainage patterns of the MOZ basin resulting in the formation of the intra-continental Okavango alluvial fan (one of the world's largest inland fan/deltas). Although the timing of initial rifting within the ORZ is not known, paleoenvironmental reconstruction suggests that feeder rivers promoted extensive flow beyond the Thamalakane and Kunyere faults circa and beyond 120,000BP into the Makgadikgadi pans (Fig. 2). However, between 120,000BP and ~ 40,000BP vertical movements along these rift-related faults caused the impoundment of the Okavango River and cutting off water supply to the pans (Ringrose, personal communication). Thus it is possible that the 40,000BP age represents a lower estimate of when active rifting was initiated within the ORZ.
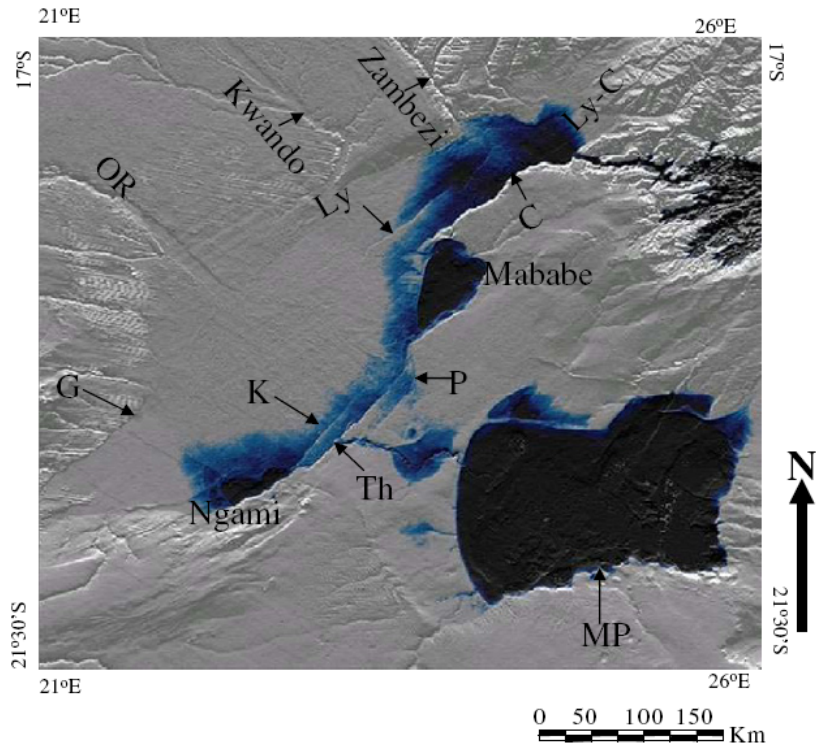
Figure 2: Shuttle Radar Topographic Mission-30 (SRTM-30) image of the study area (courtesy of Hartnady C.) showing the major rift faults and the topographic depressions. Ngami = Lake Ngami and Ly-C = Liyanti-Chobe depocenter. Th = Thamalakane, K = Kunyere, P = Phuti, C = Chobe Fault. OR = Okavango River and MP = Makgadikgadi Pans.

3. Data acquisition and processing

3.1. Aeromagnetic data

Aeromagnetic data were acquired in 1996 by the Geological Survey of Botswana. The flight elevation for the aeromagnetic data was 80 m along north-south lines with spacing of 250 m. The tie lines were east-west and spaced 1.25 km apart. The International geomagnetic reference field model of the core field was subtracted from the observed total field to get the residual total field and the data were gridded using minimum curvature technique (Briggs, 1974) with a grid cell size of 62.5 m. First and second vertical derivative filters were applied to the residual total field magnetic data in order to enhance shallow subsurface anomalies and highlight structural features such as dykes, faults and fold axes (Fig. 3a, b, and c). The depths to the top of the magnetic sources were estimated using 3 dimensional (3-D) Euler deconvolution (Thompson, 1982) in order to determine the thickness of the sedimentary fill in the rift basins and to estimate the displacements across the rift faults (e.g., Fig. 3b). A structural index of 1 was used due to pervasiveness of dykes within the study area. In our depth (fault throw) analysis, we have only used solutions with an error of less than 5%. However, we recognize that the structural index used only best approximates features resembling the dykes, therefore our depth estimates may have larger errors in areas where dykes are absent and this condition is not fulfilled. Azimuths of prominent linear features (dykes, fractures, faults, and fold axes) in the study area were measured from vertical derivative maps. The values obtained were plotted on Rose diagrams to determine the dominant orientation of structures (Fig. 4).
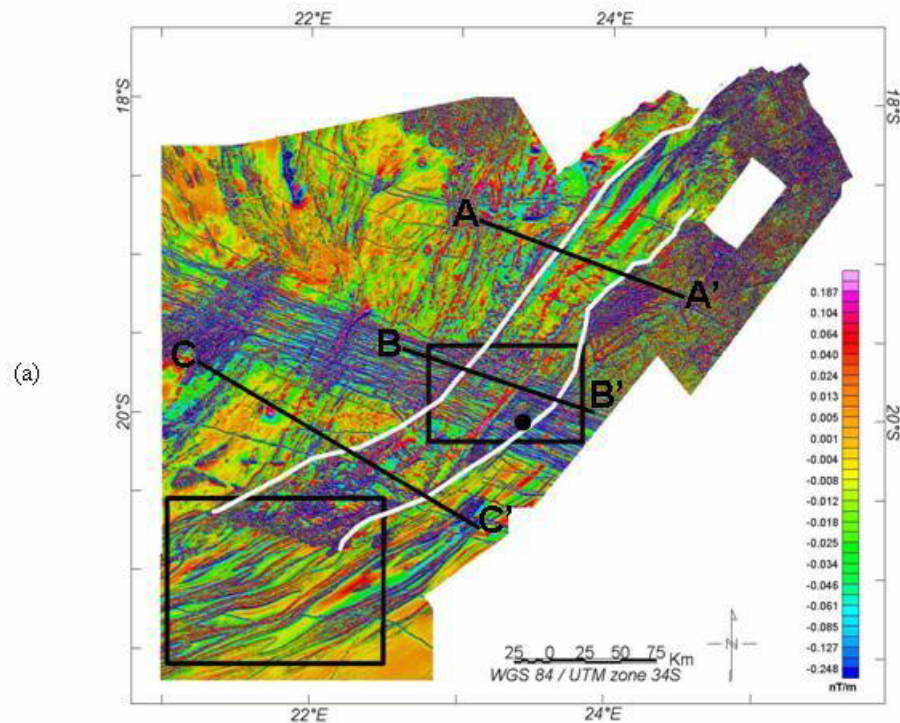
Figure 3: (a) First vertical derivative anomaly map of the Okavango Rift Zone. The boxes are areas shown on Figures 3b & c. The location of Maun is shown by a black dot. Lines show location of profiles A-A', B-B' and C-C' shown in Figure 7; (b) First vertical derivative of the magnetic anomaly map of the area shown as insert 1 in Figure 3a. Note the major rift faults trending NE-SW shown by black lines. The white line denotes profile B-B' (Fig. 7), the numbers show the depth in meters to the top of the dykes obtained from 3-D Euler deconvolution solution. T = Tsau, L = Lecha, K = Kunyere, Th = Thamalakane, P = Phuti, and N = Nare; (c) Ternary magnetic anomaly map of the area shown as insert 2 on Figure 3a. Note the detailed pattern of folding in the basement. Solid lines show the dip direction of the beds and arrows show the plunge of folding. Sekaka Shear Zone (SSZ) is shown in white.

(b)

(C)
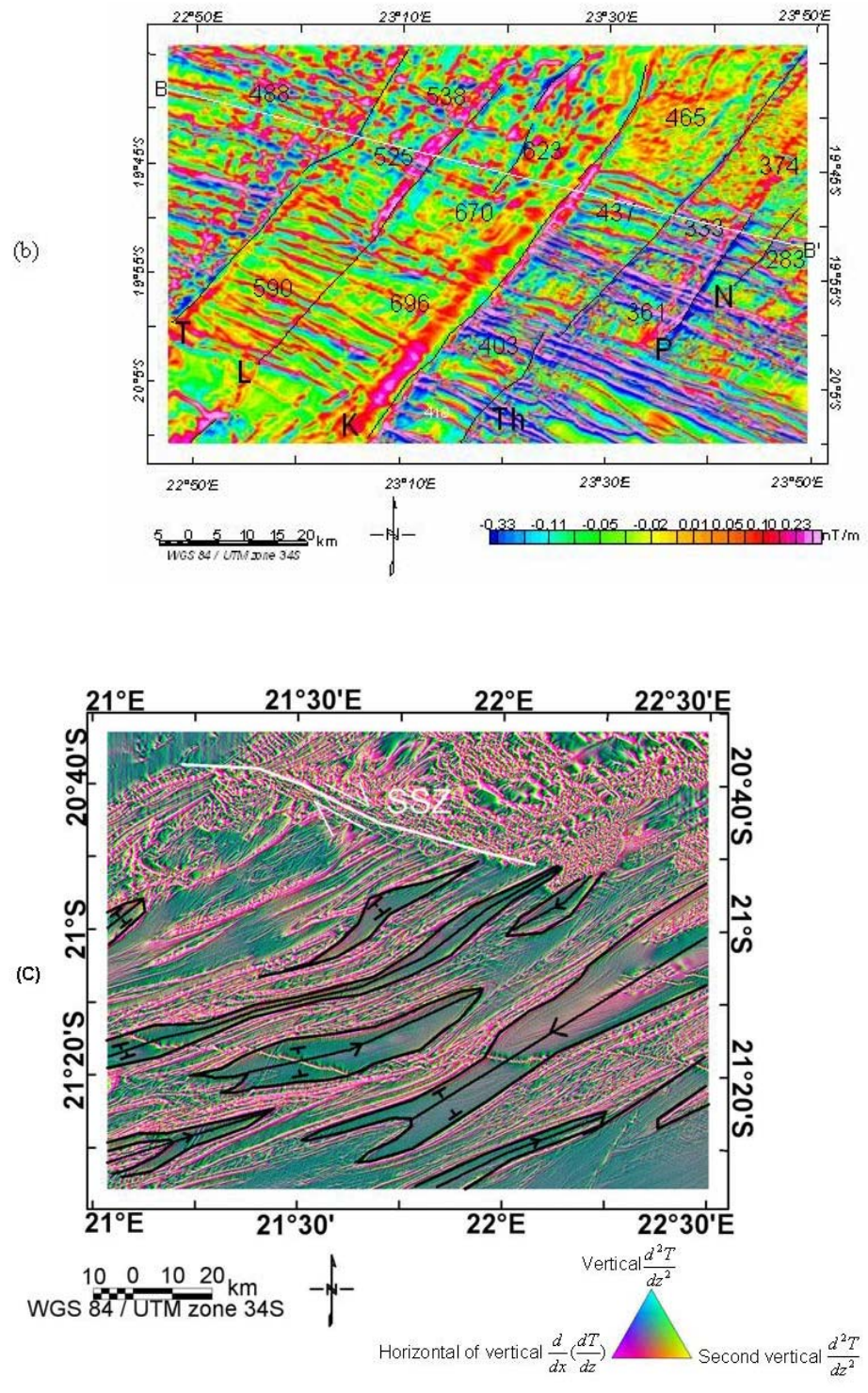
Fig. 3 (continued)

3.2. Gravity data

The gravity data were acquired by a helicopter aided survey in 1999 on a 7.5 km grid with an acquisition accuracy of 0.2 mGal. Tidal, free air and Bouguer corrections were applied to the data and the data were gridded with a grid cell size of 1.84 km using minimum curvature technique (Brigs, 1974) and a Bouguer anomaly map (Fig. 5a) prepared. In addition, 2 ¾-D gravity forward models (e.g., Fig. 5b) were constructed to determine the subsurface structure of the basin and thickness of the sediments. The models were constructed from the profile extracted from the gridded data. The forward models were prepared by approximating the shape, depth and densities that best fitted the profiles. Depths obtained from Euler deconvolution solutions were used as the initial depth estimates for the starting gravity models and the initial density values used were obtained from Telford et al., (1990) based on the lithologies underlying the rift basin as discussed in Modisi et al. (2000).
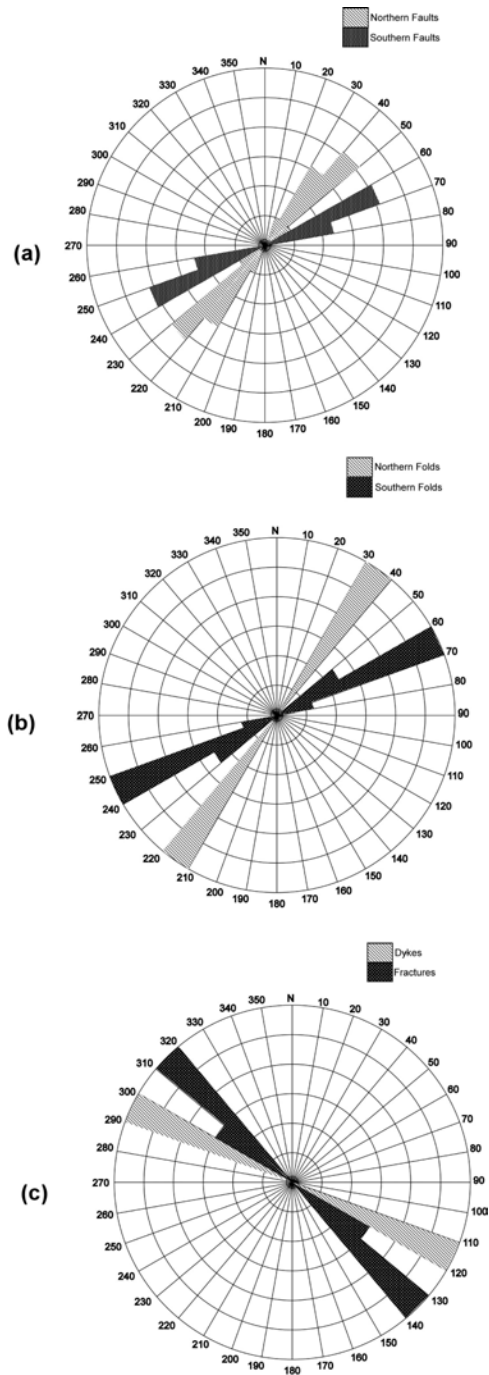
Figure 4: Rose diagrams showing plots of the (a) rift faults and (b) basement fold axes within the northern and southern sections of the study area, and (c) dykes and fractures. Note coincident azimuths of rift faults and basement fold axes.

4. Results

The vertical derivative magnetic anomaly map highlights the main structural elements of the study area (Fig. 3a). The west-northwest-trending 179 Ma Karoo dyke swarm (e.g., Fig. 3a and b) are superimposed on north-easterly trending folds (e.g., Fig. 3c) and faults of the Neoproterozoic Ghanzi-Chobe belt and are cut by younger faults associated with the rifting. These features are discussed in detail in the following sections.

4. 1. Structural Elements and Orientations

The first vertical derivative map (e.g., Fig. 3a) suggests three main fracture orientations are present in the ORZ: 1) northeast-southwest (030–070°), 2) northwest-southeast (310-320°), and 3) westnorthwest-eastsoutheast (290-300°) and are clearly visible on Rose diagrams (Fig. 4a, b, and c). The strike of the main bounding rift related faults are 030-050° in the north of the study area and 060-070° in the south (Fig. 4a). The hinge lines for folds within the basement also trend 030-40° in the north and 060-70° in the south (Fig. 4b). Therefore basement folds gradually change orientation from south (060-070°) to north (030-050°), which is the same trend followed by faults associated with the rifting (Fig. 3a).

The 310–320° structures occur within the confines of the rift forming a conjugate relationship with the 060-070° faults in the southern part of the rift zone (Fig. 3c), and also control the distributaries of the Okavango River at the distal ends of the alluvial fan (Modisi, 2000).
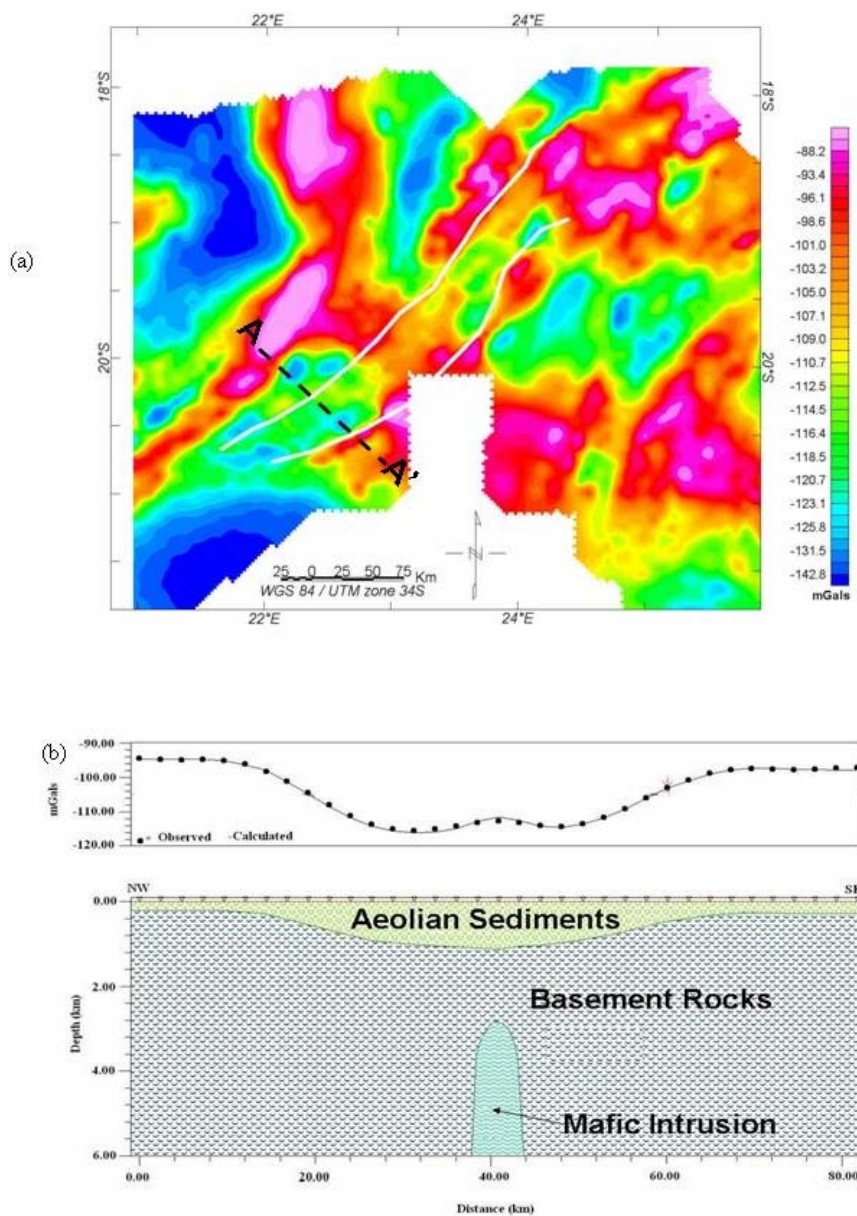
Figure 5: (a) Bouguer gravity anomaly map of the Okavango rift zone. The dashed line shows the location of profile A-A' (Figure 5b). (b) A gravity model over profile A-A' shown on Figure 5a. Note the synformal shape of the basin. Depths obtained from gravity model are similar to those obtained from magnetic 3-D Euler deconvolution solutions. Lithologic units used in the model are; Aeolian sediments (2.00g/cc), basement rocks (2.70g/cc), and mafic intrusion (2.91g/cc).

Field geologic mapping in areas where the basement is exposed in the southeastern section of the study area show that the 310–320° fractures crosscut the 060-070° foliated trends in the basement rocks (unpublished data). The 290-300° structures are typically associated with the Okavango dyke swarm and occur only within the area of the dyke swarm.

Structures found within the basement in the study area include fold belts in the southern and northern part of the study area, with the southern part of the area more pervasively covered by these basement folds (Fig. 3c). The details in the aeromagnetic map allow us to unravel the nature of the folded basement. By using a combination of depths obtained from 3-D Euler deconvolution solutions and magnetic intensity patterns, we observed that the basement is characterized by plunging folds. The higher magnetic intensity metavolcanic/volcanic rocks (e.g., the Kibaran age Kwegbe volcanics) form the cores of the antiforms and lower magnetic intensity sedimentary formations occur within the cores of synforms. The above geophysical analyses are consistent with the results of field mapping in areas where the basement rocks are exposed.

5. Discussion

5.1. Influence of Pre-existing Basement Fabric

The role of pre-existing structures and fabrics in the basement in influencing the development of continental rifts remains considerably variable from continental rift to continental rift. Several authors have suggested that the orientation of rift-related faults is strongly controlled by pre-existing basement structures (e.g., McConnell, 1972; Dunbar and Sawyer, 1988; Versfelt and Rosendahl, 1989; Ring, 1994; Modisi, 2000; Modisi et al., 2000; Mackenzie et al., 2004). In contrast, the Rukwa rift basin in Tanzania, and some parts of Turkana rift basin in Kenya within the EARS (Morley, 1999a, b) and the mid continent rift in the United States (Atekwana, 1996) are examples where the rift fabric bears no direct relationship to the basement fabrics. This leads to the suggestion that the development of continental rifts is controlled by deep-seated structures within the lithosphere (Delvaux et al., 1999). Some authors (e.g., Versfelt and Rosendahl, 1989; Morley, 1999a & b) have argued that the deviations of rift orientation from pre-rift fabrics are only at local scale and are caused by discrete, local (isolated) structures.

Within the ORZ, the potential field data show a strong correlation between the orientation of basement fabric and rift related faults. We infer from this observation that the basement fabric exerted a major influence in the development of the early rift faults within the stress regime present during initiation of the ORZ. These results are consistent with analogue and numerical models that suggest that inherited weakness zones initiate strain location, which when coupled to favorable plate kinematics can ultimately lead to continental break-up (Corti et al., 2003).

5.2. Rift boundary faults and displacements

Modisi et al. (2000) recognized several faults associated with the ORZ. The results of this investigation substantially extend this previous work by mapping the full extent of these faults as well as recognizing several new faults. The ORZ is characterized by several northeasterly trending normal faults including Gumare, Tsau, Lecha, Thamalakane, Kunyere, Phuti and Nare, Mababe, Chobe, and Liyanti (Fig. 6; Table 1). These faults define a northeast trending rift zone that extends for at least 400 km. In the south, the west-northwest trending dextral Sekaka Shear Zone (SSZ) marks the southern limit of the rift (Fig. 3c, and 6). Several of these faults (e.g., Chobe, Mababe, Liyanti, Gumare, Kunyere, Thamalakane, and Phuti) have scarps that are well defined on the Shuttle Radar Topography Model 30 (SRTM-30), Digital Elevation Models (DEM) map (Fig. 2). The Lecha, Nare, and Tsau faults lack any surface expression on the DEM maps (indicating minimal surface relief across these faults) but are well defined on the first vertical derivative (Fig. 3a & 3b) and ternary (Fig. 3c) maps.

The dip direction of these faults was determined from calculated displacements of the dykes across the faults (see Fig. 3b) similar to techniques employed by Modisi et al. (2000) and the results are presented in Table 1. Displacements across the Chobe and Liyanti faults in the northern part of the study area remain unconstrained due to limited data in this region. However, the SRTM-30 data (see Fig. 2) provide the dip direction and the full length of their exposed scarps. The Mababe Fault (>500 m throw) and the Kunyere Fault (>300 m throw) show the greatest displacements. There is also evidence of significant along strike variations in fault displacements. For example, the Kunyere Fault shows greater vertical displacements in the south (~334 m) than in the north (~286 m). In contrast, the Thamalakane Fault shows no vertical displacements in the south and an

average displacement of ~80 m along the northern extension of the fault. We infer from the displacements that the Gumare, Tsau, and Lecha faults are southeast dipping normal faults, while the Kunyere, Thamalakane, Phuti, Nare, Mababe, Liyanti, and Chobe are northwest dipping faults (Fig. 6).
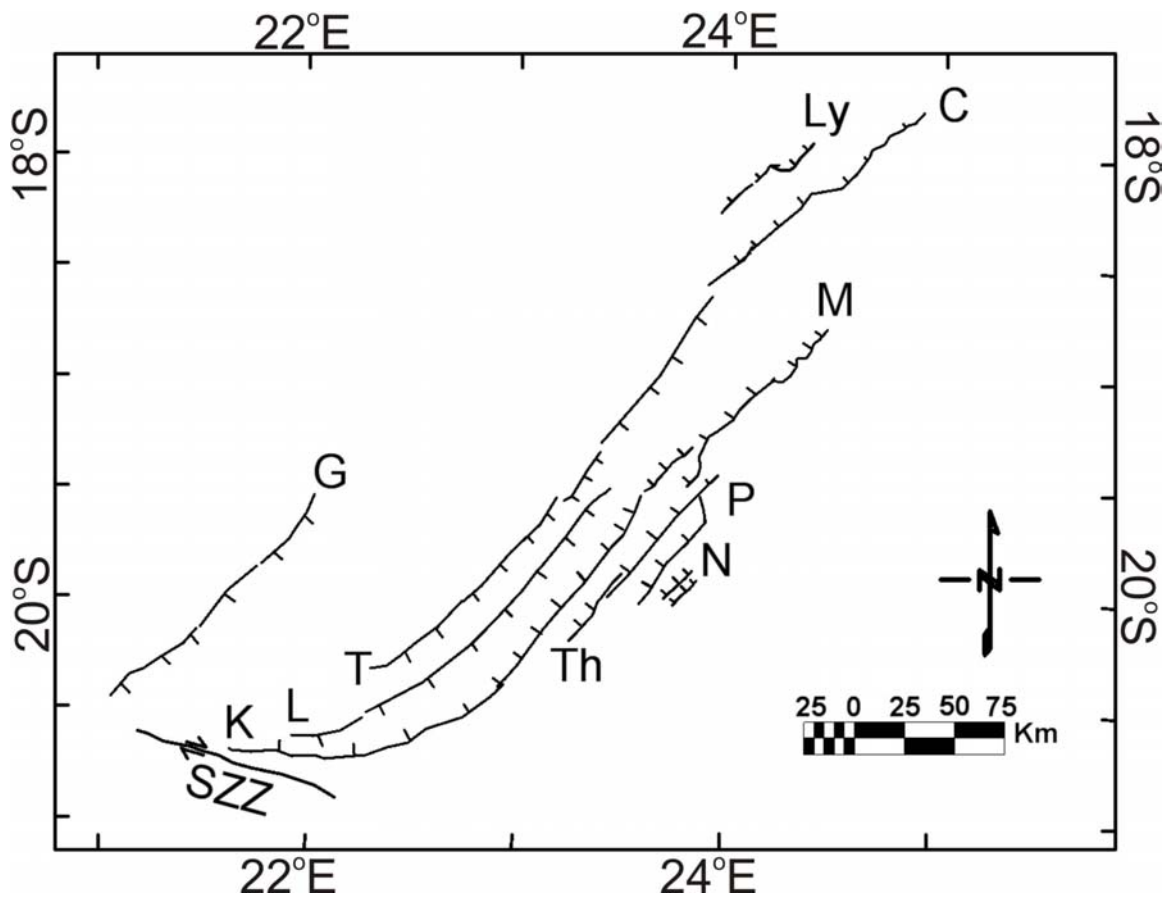
Figure 6: Major rift faults of the ORZ traced from the first vertical derivative map (Figure 2a). T = Tsau, L = Lecha, K = Kunyere, Th = Thamalakane, P = Phuti and N = Nare, SSZ = Sekaka Shear Zone. The directions of dip of the faults are shown by ticks.

Table1: Summarized values of fault vertical displacements in ORZ obtained from 3-D Euler deconvolution calculations. NA = Not Available.

Name of the fault	Throw range (m)	Approximate length (km)
Chobe	NA	150
Gumare	~17	180
Kunyere	232-334	325
Lecha	56-163	200
Liyanti	NA	50
Mababe	~521	100
Nare	~71	25
Phuti	~18	65
Thamalakane	~80	100
Tsau	43-130	225

Greater displacements consistently occur along the northwest dipping normal faults in the southeastern boundary of the rift. This suggests that these northwest dipping faults are accommodating most of the strain within the ORZ. With mostly data from the south, Modisi et al., (2000) concluded that the Kunyere Fault was the main boundary fault of this rift zone. This study confirms this to be the case only in the southern portion of the rift in the vicinity of Lake Ngami. Towards the north, displacement along the

Kunyere Fault wanes and the main displacement is recorded along the Mababe Fault making the later the main boundary fault within the Mababe Graben (Fig. 2).

The Gumare and Nare faults appear to represent the northwest and southeast extent of recognized rift-related faults and define a zone of extension about 150 km wide. However, most of the active subsidence is taking place within a zone ~ 50 -60 km wide along the southeastern boundary of the rift defined by three main depocenters, L. Ngami, Mababe, and Liyanti-Chobe (Fig. 2). This suggests the development of an active rift within a larger rift forming a rift-in rift structure. The limits of the grabens are defined by: (a) the Tsau and Kunyere faults in the L. Ngami area; (b) the Tsau and Mababe faults in the Mababe area; and (c) the Chobe and possible extension of the Gumare Fault in the Linyanti-Chobe area. It is important to note that a micro- earthquake study conducted in this area in 1974 revealed that seismic activity was largely limited to the southeastern boundary of the rift zone and associated with the northwest dipping faults (Kunyere, Thamalakane, Mababe, and Chobe) and focused mostly within the L. Ngami, Mababe, and Liyanti-Chobe depocenters/grabens (Scholz et al., 1976). We infer from this observation that the localization of strain resulting from extension is occurring mostly along the southeastern boundary where the border system is being initiated, underscoring the important role of border faults in accommodating strain even during this incipient stage of rift development. This interpretation is consistent with the results of studies that suggest that border faults play a dominant role in localizing strain during the early stages of continental rifting (e.g. Ebinger and Casey, 2001; Ebinger et al., 2004; Keranen et al., 2004).

5.3. Basin geometry and development in relation to border faults

Three schematic cross-sections across the northern, central, and southern portions of the ORZ, provide insight into the early geometry of this incipient rift zone (Fig. 7). Greater subsidence in the ORZ is observed along both the southern (C-C') and northern profiles (A-A'). Within the L. Ngami area (profile C-C') the greatest vertical displacement occurs along the Kunyere Fault (~334 m) as compared to the Tsau Fault (~130 m). Within the Mababe area (A-A'), the Mababe Fault shows ~521 m of displacement compared to the Tsau Fault (~114 m). The presence of well developed graben structures at Ngami and Mababe can account for this greater accumulation of sediment (Fig. 7). The depth to basement shallows along profile B-B' in the central portion of the ORZ. Here the Kunyere Fault again has a greater displacement (~232 m) compared to the Tsau Fault (100 m). A graben structure is also inferred to underlie the central portion of the rift. We speculate that the presence of the Karoo dyke swarm in this location has significantly changed the overall mechanical (strength) properties of the crust and this difference is reflected in the apparent reduction in the amount of crustal extension and development of the depocenters overlying grabens within the ORZ.
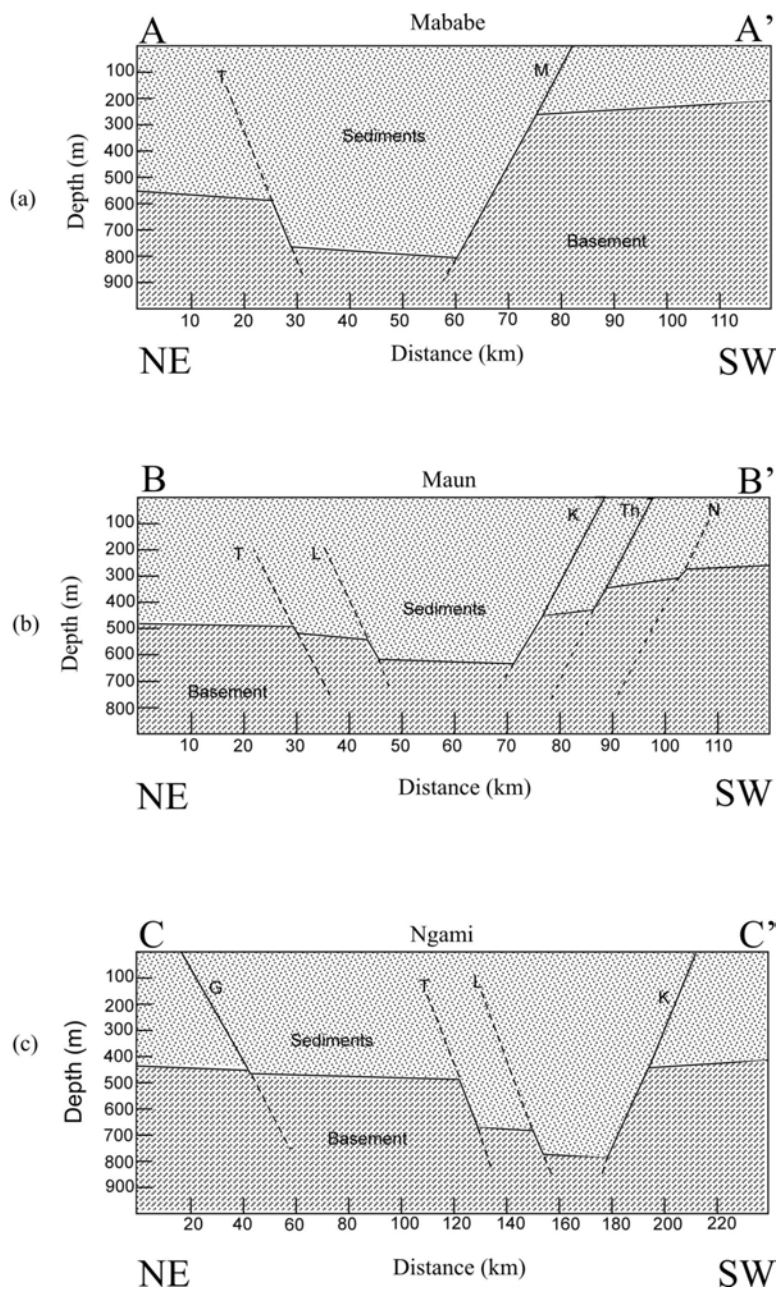
Figure 7: Cross sections constructed from the depths to the top of dykes to show rift fault throws. Doted lines indicate that the depth extent of fault is not known. T = Tsau, L = Lecha, K = Kunyere, Th = Thamalakane, P = Phuti and N = Nare. Profile locations are shown on Figure 2a. Note that the effect of the vertical exaggeration on the dip of the faults is ignored in order to preserve the shape of the basins.

The 2-D basin geometry and the shallow subsurface structure of the rift was also investigated using gravity models constructed along three profiles taken perpendicular to the long axis of the rift (Fig. 5). Gravity models yield similar results to the cross-sections constructed on the basis of the magnetic signature of the rift and one example is shown for comparison (Fig. 5b). This negative anomaly has an intra basin residual positive anomaly with amplitude of 5 mGal (Fig.5b) a feature that is characteristic of gravity profiles from East Africa (e.g., Baker and Wohlenberg, 1997). A possible interpretation of this intra basin positive anomaly is that it is due to a mafic intrusion within basement rocks. Alternatively, the anomaly can equally be explained in terms of topographic changes (i.e. the presence of a horst block) within the rift basin. In order to test whether this intrusion and the associated positive anomaly is deep or shallow seated, upward continuation filters were applied to the data at elevations of 1, 2.5, and 5 km. The upward continuation of data enhances deep-seated features (e.g., a mafic intrusion) at the expense of shallow features. Upward continuation at an elevation of 5 km did not show the anomaly suggesting that the intrusion is shallow, and may be more consistent with the presence of a central basement horst. On the basis of the gravity model, the shape of rift basin appears to be a synformal depression with both flanks raised (Fig. 5b) rather than a half-graben. Half-graben geometry is common of many rift grabens forming the EARS. However, the vertical exaggeration for our models may not have the sensitivity to resolve small differences in vertical displacements (~100-~300) typical of the faults near L. Ngami where the profile was taken. Morley (2002) has suggested that half-grabens evolve through different stages (e.g., Fig. 8): (a) an early rift stage characterized by a synformal depression; (b) an early half-graben stage, where the border fault is being

initiated; (c) a mature half-graben stage with a well developed border fault; and (d) a late-stage half-graben. Morley's model suggests that in basins where basin development precedes significant border fault development, half-grabens evolve from synformal depressions as the border fault is being initiated (e.g., from stage a to stage b; Fig. 8). Greater displacements along the NW dipping Kunyere and Mababe faults when compared to the SE dipping Tsau Fault suggests an early half-graben development stage (e.g., stage b; Fig. 8) for the ORZ. In the Mababe Graben, the Mababe Fault shows more than four times the displacement observed on the SE dipping Tsau Fault suggesting a more advanced stage of development for this graben compared to the L. Ngami graben. However, we have yet to find evidence supporting the presence of a fully developed half-graben in the ORZ. This implies that the border fault system which includes the Kunyere and Mababe faults may not be fully developed. Thus, we speculate from this observation that in the ORZ, local border faults and grabens are developing simultaneously and have yet to link up to establish a master border fault that controls the development of the rift on a regional scale.
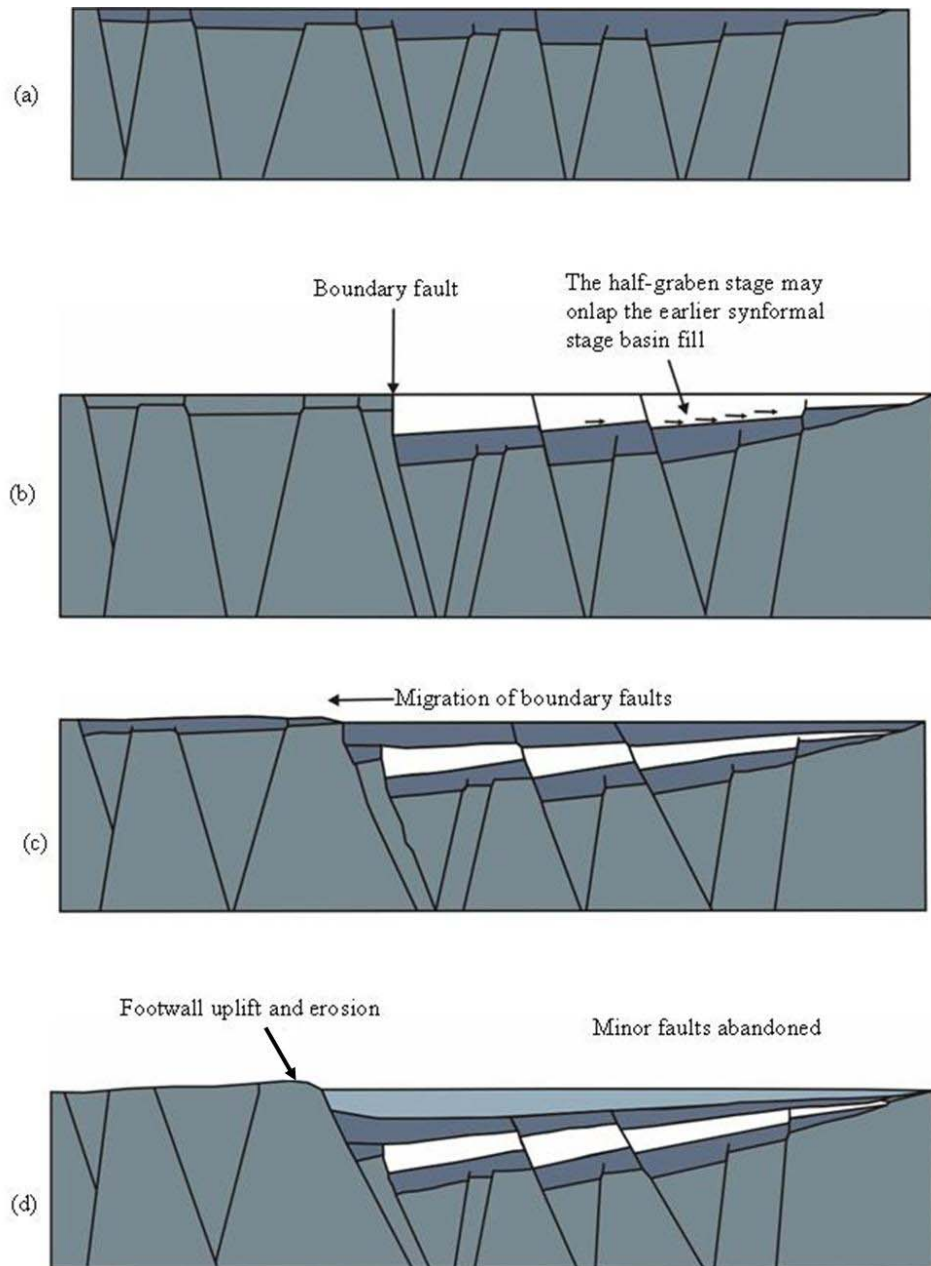
Figure 8: Schematic diagram showing the evolution of the rift zone from a synformal basin to half-graben. (a) early rift stage, synformal depression; (b) early half-graben stage-development of boundary fault; (c) mature half-graben; and (d) late-stage half-graben. Okavango Rift Zone is suggested to be in transitional stage between (a) and (b) (redrawn from Morley, 2002).

6. Conclusion

An aeromagnetic and gravity data analysis of the ORZ has resulted in the following conclusions: (1) the basement fabric played an important role in localizing the development of faults within the stress regime present during the initiation of this rift, (2) three *en échelon* northeast trending depocenters/grabens define the ORZ (L. Ngami, Mababe, and Liyanti-Chobe), (3) this early rift stage is characterized by a synformal depression to early half-graben stage lacking a well developed border fault system consistent with the early stages in the evolution of half-grabens, (4) boundary faults along the southeastern boundary of the rift accommodate most of the strain defining a 50 km wide zone of subsidence within a larger 150 km wide zone of forming a rift-in rift structure. The above observation highlights the important role of border faults, even within localized regions, in accommodating strain even during this incipient stage of rifting.

References

Atekwana, E. A., 1996. Precambrian basement beneath the central mid continent United States as interpreted from potential field imagery. Basement and basins of Eastern North America. Geological Society of America. Special Paper 308, 33–44.

Ballard, S., Pollack, H. N., Skinner, N. J., 1987. Terrestrial heat flow in Botswana and Namibia: Journal of Geophysical Research 92, 6291-6300.

Baker B. H., Wohlenberg, J., 1971. Structure and Evolution of the Kenya Rift Valley. Nature 229, 538-542.

Bastow, I. D., Stuart, G. W., Kendall, J. M., Ebinger, C. J., Ayele, A., Cornwell. D. G., Maguire, P. K. H., 2004. Upper mantle seismic structure of the Northern Main Ethiopian Rift-a region of incipient continental breakup. In: Yirgu, G., et al., (Eds.), Proceedings of International Conference on East Africa Rift System, June 20-24, 2004, Addis Ababa, Ethiopia: Ethiopian Geoscience and Mineral Engineering Association, pp. 30-33.

Briggs, I. C., 1974. Machine contouring using minimum curvature. Geophysics 39, 39-48. Chapman, D. S., Pollack, H. N., 1977. Heat flow and heat production in Zambia: Evidence for lithosphere thinning in central Africa. Tectonophysics 41, 79-100.

Chorowicz, J., 2005. The East African rift system. Journal of African Earth Sciences 43, 379- 410.

Cooke, H. J., 1984. The evidence from northern Botswana of climate change. In: Vogel, J. (Eds.), Late Cenozoic palaeoclimates of the southern hemisphere. Balkema, Rotterdam, pp. 265 278.

Corti, G., Van Wijk, J., Bonini, M., Sokoutis, D., Cloetingh, S., Innocenti, F., Manetti, P., 2003. Transition from continental break-up to punctiform seafloor spreading: How fast, symmetric and magmatic. Geophysical Research Letters 30, 12, 1604, doi: 10.1029.

Delvaux, D., Fronhoffs, F., Hus, R., Poort, J., 1999. Normal fault splays and transfer zones in the central part of the Baikal rift basin: Insight from digital photography and bathymetry. Bull. Centres Rech. Explor. Prod. Elf Aquitaine 22, 2, 341-358.

Dunbar, J. A., Sawyer, D. S., 1988. Continental rifting at pre-existing lithospheric weaknesses. Nature 333, 450-452.

Ebinger, C. J., Rosendahl, B., Reynolds, D., 1987. Tectonic model of the Malawi Rift, Africa. In: Ben-Avraham, Z., (Eds.), Sedimentary basins within the Dead Sea and other rift zones. Tectonophysics 141, 215-235.

Ebinger, C. J., 1989. Tectonic development of the western branch of the East African Rift System. Geological Society of America Bulletin 101, 885-903.

Ebinger, C. J., Casey, M., 2001. Continental breakup in magmatic provinces: An Ethiopian example. Geology 29, 6, 527-530.

Ebinger, C., Wolfenden, E., Keir, D., Yirgu, G., Ayele, D., Casey, M., Waltham, D., EAGLE Working Group, 2004. Incipient continental breakup in northern Ethiopian rift: No need for detachment faults. In: Yirgu, G, et al., (Eds.), Proceedings of International Conference on East Africa Rift System, June 20-24 2004, Addis Ababa, Ethiopia: Ethiopian Geoscience and Mineral Engineering Association, pp. 58-60.

Fairhead, J. D., Girdler, R. W., 1969. How far does the rift system extend through Africa? Nature 221, 1018-1020.

Girdler, R. W., 1975. The great Bouguer anomaly over Africa. Eos (Transactions, American Geophysical Union) 56, 516-519.

Gumbricht, T., Mc Carthy, T. S., Merry, C. L., 2001. The topography of the Okavango Delta, Botswana, and its tectonic and sedimentological implications. Journal of Structural Geology 104, 243-264.

Kampunzu, A. B., Bonhomme, M. G., Kanika, M., 1998. Geochronology of volcanic rocks and evolution of the Cenozoic Western branch of the East African rift system. Journal of African Earth Sciences 26, 441-461.

Keranen, K., Klemperer, S. L., the EAGLE Working Group., 2004. 3D seismic imaging of protoridge axis in the Main Ethiopian Rift. Geology, 32, 11, 949-952.

Mackenzie, G. D., Thybo, H., Maguire, P. K. H., Ebinger, C. J., the EAGLE Working Group, 2004. Evidence for crustal structure influence on the evolution of the Main Ethiopian Rift. In: Yirgu, G., et al., (Eds.), Proceedings of International Conference on East Africa Rift System, June 20-24 2004, Addis Ababa, Ethiopia: Ethiopian Geoscience and Mineral Engineering Association, pp. 130-133.

McCarthy, T. S., Green, R. W., Franey, N. J., 1993. The influence of neo-tectonics on water disposal in the northeastern regions of the Okavango swamps, Botswana. Journal of African of Earth Sciences 17, 1, 23-32. McConnell, R. B., 1972. Geological development of the rift system of eastern Africa. Geological Society of America Bulletin 83, 2549-2572.

Modisi, M. P., 2000. Fault system of the southeastern boundary of the Okavango Rift, Botswana. Journal of African Earth Sciences 30, 569-578.

Modisi, M. P., Atekwana, E. A., Kampunzu, A. B., Ngwisanyi, T.H., 2000. Rift kinematics during the incipient stages of continental extension: Evidence from the nascent Okavango rift basin, northwest Botswana. Geology 28, 939-942.

Moore, A. E, Larkin, P., 2001. Drainage evolution in south-central Africa since the breakup of Gondwana. South African Journal of Geology 104, 47-68.

Morley, C. K., 1999a. How successful are analogue models in addressing the influence of pre-existing fabrics on rift structure? Journal of Structural Geology 21, 1267-1274.

Morley, C. K., 1999b. Influence of pre-existing fabrics on rift structure. In: C.K. Morley (Eds.), Geoscience of Rift Systems–Evolution of East Africa. American Association of Petroleum Geologist, Studies in Geology 44, 151-160.

Morley, C. K., Ngenoh, D. K., Ego, J. K., 1999. Introduction to the East African Rift System. In: C.K. Morley (Eds.), Geoscience of Rift Systems–Evolution of East Africa. American Association of Petroleum Geologists, Studies in Geology 44, 1-18.

Morley, C. K., 2002. Evolution of large normal faults: Evidence from seismic reflection data. American Association of Petroleum Geologist Bulletin, 6, 961-978.

Nyblade, A. A., Owens, T. J., Gurrola, H., Ritsema, J., Langston, C.A., 2000. Seismic evidence for a deep mantle thermal anomaly beneath east Africa. Geology 28, 7, 599-602.

Owens, T. J., Nyblade, A. A., Gurrola, H., Langston. C. A., 2000. Mantle transitions zone beneath Tanzania, East Africa. Geophysical Research Letters 27, 6, 827-830.

Reeves, C. V., 1972. Rifting in the Kalahari? Nature 237, 95–96.

Ring, U., 1994. The influence of preexisting structure on the evolution of the Cenozoic Malawi rift (East African rift system). Tectonics 13, 313-326.

Ringrose, S., Kampunzu, A.B., Vink, B., Matheson, W., Downey, W., 2002. The origin and paleoenvironments of calcareous sediments in Moshaweng dry valley, southeast Botswana. Earth Surface Processes and Landforms 27, 591-611.

Rosendahl, B. R., 1987. Architecture of the continental rifts with special reference to East Africa. Annual Reviews of Earth and Planetary Sciences 15, 445-503.

Russell, L. R., Snelson, L. 1994. Structural style and tectonic evolution of the Albuquerque Basin segment of the Rio Grande Rift, New Mexico, U.S.A. In: S. M. Landon (Eds.), Interior Rift basins. American Association of Petroleum Geologists 59, 205-258.

Sebagenzi, M. N., Vasseur, G., Louis, P., 1993. First heat flow density determinations from southeastern Zaire (central Africa). Journal of African Earth Sciences 16, 413-423.

Sebagenzi, M. N., Kaputo K., 2002. Geophysical evidences of continental break up in the southeast of the Democratic Republic of Congo and Zambia (Central Africa). In: S. A. P. L. Cloetingh, and Z. Ben-Avraham (Eds.), From continental extension to collision: Africa- Europe interaction, the Dead Sea and analogue natural laboratories. EGU European Geosciences Union, Stephan Mueller Special Publication Series 2, 193-206.

Scholz, C. H., Koczynski, T. A., Hutchins, D. G., 1976. Evidence for incipient rifting in southern Africa. Royal Astronomical Society Geophysical Journal 44, 135-144.

Telford, W. M., Geldart, L. P., Sherrif, R. E., 1990. Applied Geophysics, Second edition. Cambridge University Press, NY, 770p.

Thomas, D. S. G., Shaw, P. A., 1991. The Kalahari environment. Cambridge University Press, Cambridge, UK, 324p.

Thompson, D. T., 1982. EULDPH - A technique for making computer-assisted depth estimates for magnetic data. Geophysics 47, 31-37.

Versfelt, J., Rosendahl, B. R., 1989. Relationships between pre-rift structure and rift architecture in lakes Tanganyika and Malawi, East Africa. Nature 337, 354-357.

2. FAULT GROWTH AND PROPAGATION DURING INCIPIENT CONTINENTAL RIFTING: INSIGHTS FROM A COMBINED AEROMAGNETIC AND SRTM DEM INVESTIGATION OF THE OKAVANGO RIFT ZONE, NW BOTSWANA

*Kinabo[a], B. D., Hogan[a], J. P., Atekwana [b], E. A., Abdelsalam[a], M. G., Modisi[c], M. P.

[a]University of Missouri-Rolla, Department of Geological Sciences and Engineering, 129 McNutt Hall, Rolla, MO 65409 USA

[b]Oklahoma State University, Boone Pickens School of Geology, 105 Noble Research Center, Stillwater, Oklahoma, 74078 USA

[c]Department of Geology, University of Botswana, Private Bag 0022, Gaborone, Botswana

Abstract

Digital Elevation Models (DEM) extracted from the Shuttle Radar Topography Mission (SRTM) data and high resolution aeromagnetic data are used to characterize the growth and propagation of faults associated with the early stages of continental extension in the Okavango Rift Zone (ORZ), NW Botswana. Faults are recognized on the DEM by their topographic scarps and on the aeromagnetic maps as thin magnetic lineaments truncating the Karroo dikes and by abrupt changes in magnetic intensity. Significant differences in the height of fault scarps and the throws across the faults indicate extended fault histories accompanied by sediment accumulation within the rift graben. Basement faults that lack topographic expression are present near the center of the rift and appear to be inactive, faults with large throws and small scarp heights indicate waning activity, faults with large throws and significant scarp heights are older and active, and faults where the throw and scarp height are in closer agreement are considered young and active. Individual faults grow first by soft linkage (under lapping to overlapping segments,) to hard linkages (hooking, fused segments). Major faults have linked together to establish an immature border fault. This maturation process results in both lengthening and widening of the topographic rift basin. The orientation of river/stream channels coincides with the expressions of faults and/or fractures implying coupling of neo-tectonic and fluvial processes. Integration of these two datasets provides a 3-D view of the faults and fault systems, providing new insight into fault growth and propagation during the nascent stages of rifting.

Keywords: Fault linkages, border faults, Okavango Rift Zone, incipient rifts, coupling SRTM (DEM)-aeromagnetic data.

1. Introduction

The location, orientation, and evolution of normal faults that form during continental rifting exert a strong influence on the development of regional features of the rift including: 1) geomorphology, 2) drainage patterns, 3) basins location, 4) stratigraphy, 5) location of magmatism, and if the process of continental rifting is successful, 6) the geometry of the passive margin. Understanding the factors which control the growth and propagation of normal faults at the earliest stages of continental rifting will lead to a better overall understanding of the processes which control the development of continental rifts – an essential component of the plate tectonics paradigm. Additionally, because rift basins and rifted continental margins are considered to be the most prolific areas of hydrocarbon accumulation *[Trudgill and Underhill*, 2002] this knowledge can lead to increased efficiency in petroleum exploration and the development of proven reserves. Our understanding of the earliest stages of fault development and the details of fault linkage and propagation during continental rifting is still limited mainly because we can only study the present-day geometry of the faults [*Schlische and Anders*, 1996]. Investigation of continental rifting has typically focused on a few well documented continental rifts (e.g., the East African Rift System (EARS), Baikal Rift, and Rio Grande Rift) where border faults are either fully developed or in an advanced stage of development. Furthermore, observations critical to constraining processes important to the early stages of fault development during continental rifting are commonly made obscure in these more mature rifts by accumulation of thick sedimentary sequences, volcanic sequences or by poly-phase deformation related to continued rifting. There exist only a few examples of young continental rifts which are suitable for the investigation of

the process of border fault development and evolution. The Okavango Rift Zone (ORZ), in northwest Botswana (Fig. 1) is such a zone of incipient continental rifting [*Scholz et al.*, 1976; *Modisi et al.*, 2000]. Recent studies suggest that faults associated with this rift are still in a juvenile stage [*Kinabo et al.*, 2007]. Thus, the ORZ can serve as a modern day analogue for the earliest stages of more evolved continental rift basins and provides us with a unique opportunity to investigate the earliest developmental stages of continental rifts such as fault growth and propagation.

Studies on fault growth and evolution have traditionally relied on field studies such as structural mapping and stratigraphic analysis, analogue models using sand and clay experiments, and numerical models to understand formation, early interactions of segments and growth of the faults [*Cowie,* 1992, 1998b*; Trudgill and Cartwright*, 1994; *Cartwright et al.,* 1995; *Mulugeta and Woldai*, 2001; *Moustafa, 2002*; *Withjack, 2002*]. Alternative studies have used an integration of seismic data analysis and field work [e.g., *Morley 2002*; *Davis et al.*, 2000] or a combination of analogue models/ numerical models with fieldwork for understanding fault growth and propagation and their effect on stratigraphic architecture and dispersal patterns [e.g., *Mc Clay et al.,* 2002]. However, in areas where the faults are mostly buried beneath large accumulations of sediment, have subdued surface relief, or where access and travel is limited, such as in the case of ORZ [*Kinabo et al.*, 2006; *Modisi et al.*, 2000], it is difficult to accomplish structural mapping, stratigraphic analysis, and seismic studies through land based field work. For such areas (which would include planetary bodies), important structural information regarding rift processes can be gleaned from magnetic data [*Modisi et al.* 2000; *Grauch,* 2000]. Other studies including *Macheyeki et al.* [2005] and *Kervyn et al.* [2006] have also shown the

utility of Digital Elevation Models (DEM) to map rift fault morphology. In this study we couple SRTM DEM data (which provide surface morphology of the faults) with high resolution aeromagnetic data (which provide information about the fault within the basement) to provide a three dimensional perspective of faults and fault patterns associated with ORZ. We use this information to: (1) examine all stages of fault linkage, growth, and propagation within the ORZ, (2) investigate the emergence of a master-border fault system, and (3) demonstrate the utility of coupled SRTM DEM – high resolution aeromagnetic data to provide important insights into the process of fault propagation, linkage, and growth and development of border fault systems in this incipient continental rift zone.
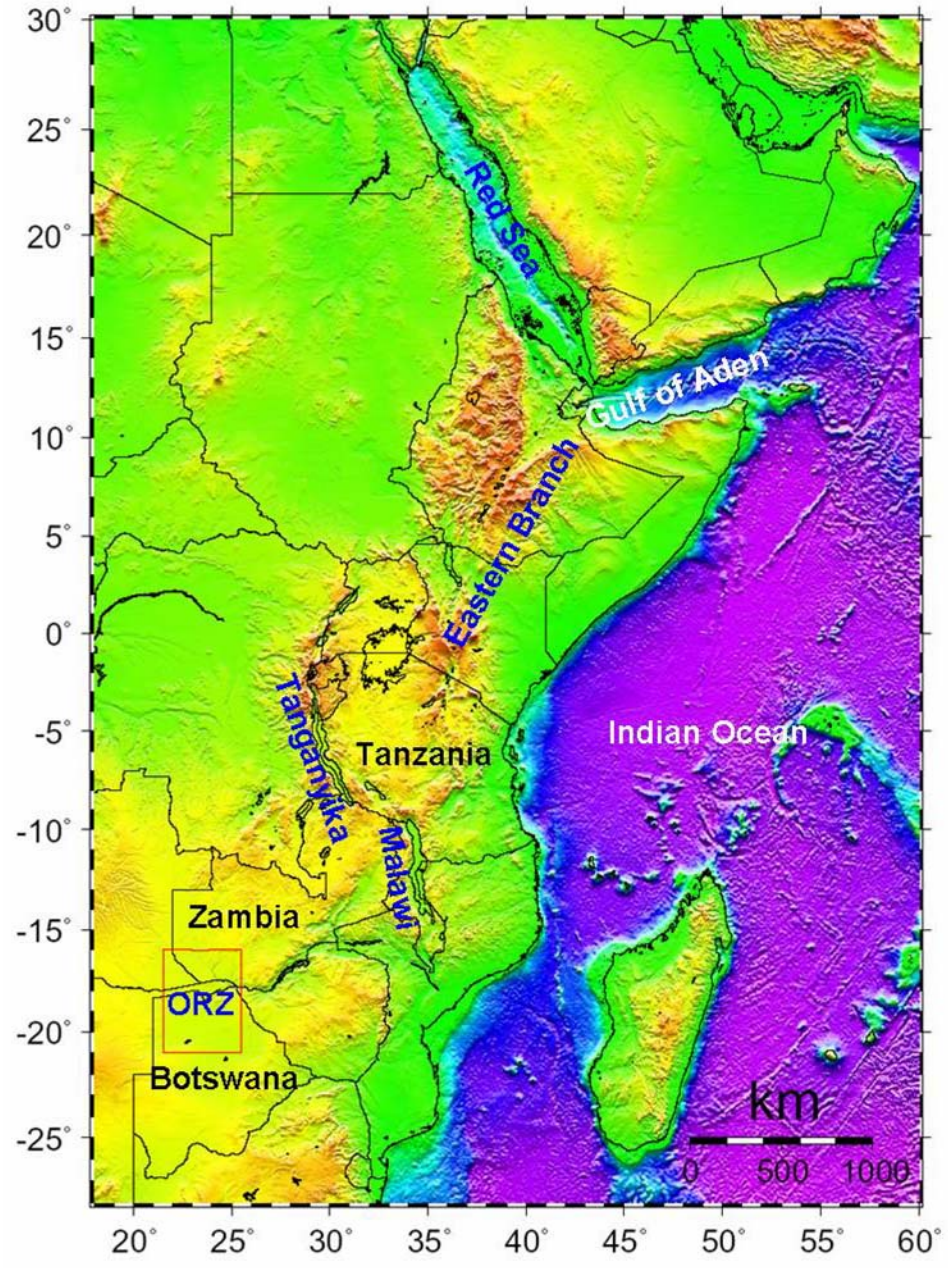
Figure 1: SRTM DEM map of the East Africa Rift System showing the location of the study area (red rectangle).

2. The Okavango Rift Zone

The Okavango basin in NW Botswana is located at the southern tip of the southwestern branch of the EARS (Fig. 1). The basement geology in this area is mostly buried underneath 200-300 m of the Kalahari sediments and very few outcrops are exposed in the northern and southern part of the ORZ [*Modisi et al.*, 2000; *Kinabo et al.*, 2007]. A micro-earthquake study conducted in 1974 revealed that this is an area of incipient rifting with active Quaternary to Recent NE-trending normal faults [*Scholz et al.*, 1976]. The ORZ can be subdivided into three grabens, from SE to NE they are, Lake Ngami, the Mababe Depression, and the Liyanti-Chobe (Fig. 2).

Several lines of evidence can be used to constrain the age for initiation of rifting in ORZ. Rifting began after the 179 Ma Karoo dike swarm [Le Gall et al., 2002] which is displaced by the rift faults (see Fig. 3c). Paleoenvironmental records suggest that feeder rivers of the Okavango system promoted extensive wet and dry conditions beyond the Thamalakane and Kunyere Faults circa and prior to 110 ka into the Makgadikgadi pans (Fig. 2). However, ~41 ka vertical movements along rift-related faults caused impoundment of the Okavango River, cutting off water supply to the pans [*Ringrose et al.*, 2005] suggesting that the 41ka age represents the best estimate for initiation of active rifting within the ORZ.

Modisi et al., [2000] using high-resolution aeromagnetic data over the southern portion of the ORZ documented that the width of this rift is similar to that of the more mature basins of the EARS and that pre-existing basement structures exert a major control over the rift development. Kinabo et al., [2007] using a more complete gravity and aeromagnetic geophysical database of the ORZ examined the full extent of the rift

structures and confirmed a strong influence of pre-existing basement fabrics on localization and development of rift related faults and established that the shape of the rift graben is a synformal to half-graben. This study extends the investigation of the two previous studies by focusing on the details of fault propagation, linkage, and growth, and the development of border faults during the early stages of continental rifting.
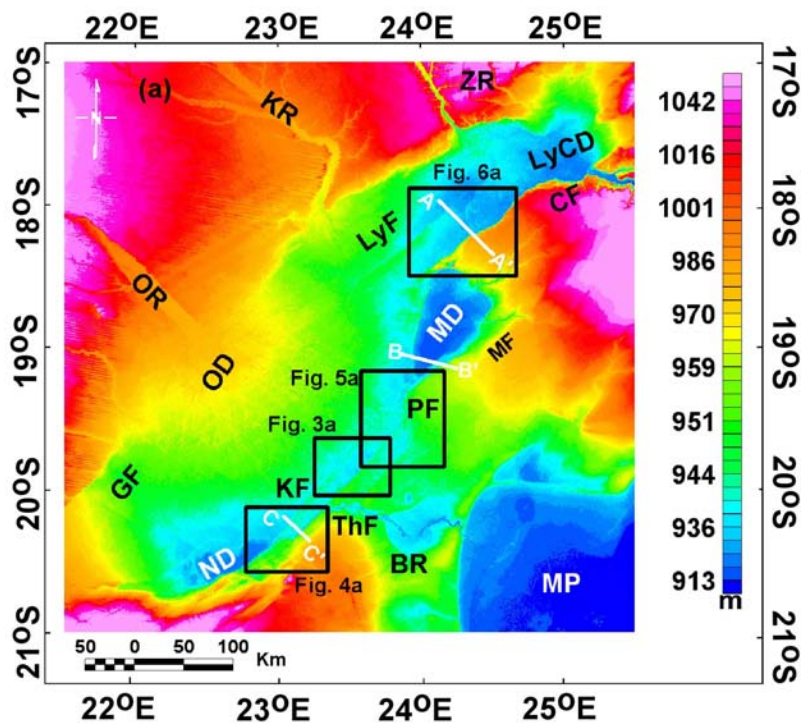
Figure 2 (a): SRTM DEM map of the Okavango Rift Zone showing major rift faults and depocenters. GF = Gumare Fault, KF = Kunyere Fault, ThF = Thamalakane Fault, PF = Phuti Fault, MF = Mababe Fault, CF = Chobe Fault, LyF = Linyanti Fault, MP = Makgadikgadi Pans, ND = Ngami Depression, LyCD = Linyanti-Chobe Depression, MD = Mababe Depocenter, ZR is Zambezi River, OD = Okavango Delta, OR = Okavango River, and KR = Kwando River. The areas shown in boxes are shown in Figures 3-6 and white lines are profiles shown in Figure 9. (b) Structural map of the ORZ interpreted from aeromagnetic and SRTM DEM data (black lines). The faults in red were interpreted from aeromagnetic data alone and faults in blue were interpreted from SRTM DEM data alone. The ticks on the faults indicate the fault dip azimuth. Symbols are same as in Figure 2a.
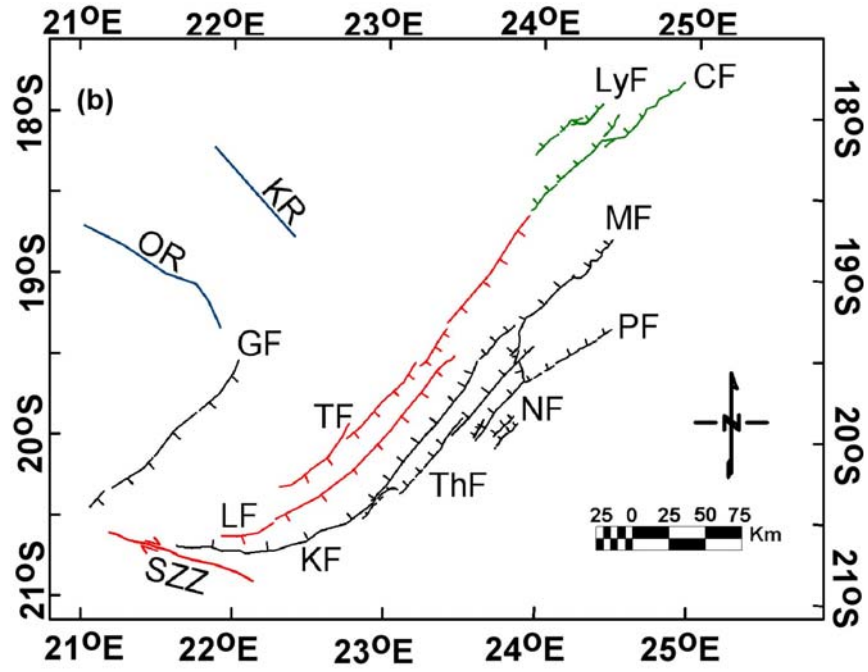
Fig. 2 (continued)

3. Data Acquisition and Processing

3.1 Shuttle Radar Topography Mission, Digital Elevation Model (SRTM DEM)

The February, 2000 Shuttle Radar Topography Mission (SRTM) was a joint international project between the United States National Geospatial-Intelligence Agency (NGA) and the National Aeronautics and Space Administration (NASA), and the German and Italian Space Agencies. SRTM DEM is distributed by NASA's Jet Propulsion Lab (JPL) in $1^{o}x1^{o}$ tiles. Two types of SRTM data are available: one arc data (SRTM-1, 30 m X-Y resolution); and three arc data (SRTM-3, 90 m X-Y resolution and ± 30 m root mean square error z accuracy). Only SRTM 3 data are available for Africa and, therefore, are used in this study. Data were analyzed using ENVI (ITT, Visual Information Solutions, 2004). Data scenes were combined to form a mosaic and registered using image-to-image technique [Chen and Lee, 1992]. Visual interpretations of SRTM DEM are shown in the form of structural maps illustrating the strike, dip direction, and spatial distribution of these faults and related structures (Fig 3b, 4b, 5b, and 6b). Topographic profiles were extracted from SRTM DEM data from selected areas to document the morphology associated with surface rupture of the rift faults. Three topographic profiles were extracted across the selected lineaments to demonstrate a consistent existence of fault scarps (the profile are 4-14 km apart). A moving average of 20 data points was applied to filter out above ground features such as trees and boulders (Fig. 9). Throughout our discussion we will use DEM to represent SRTM DEM.
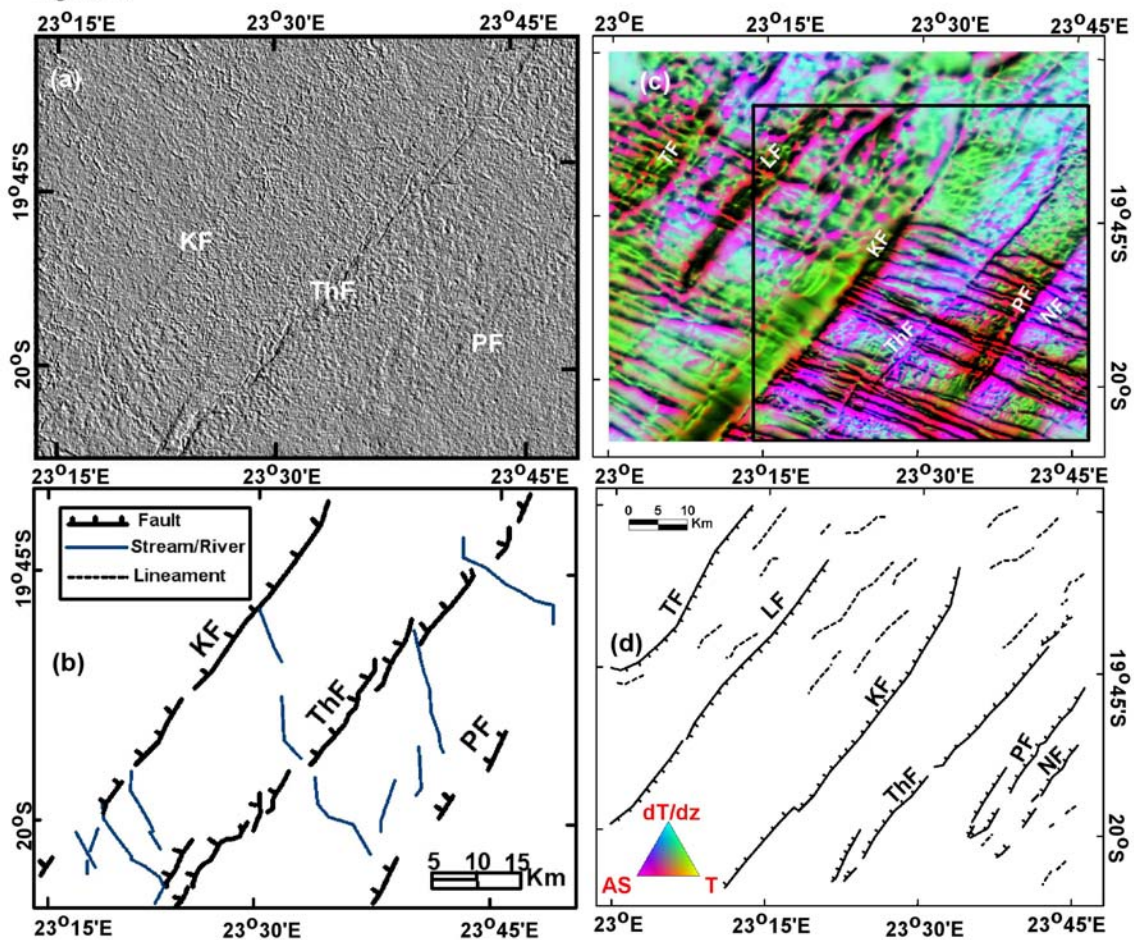
Figure 3: (a) Hill shade SRTM DEM map showing isolated segments along the Kunyere Fault and overlapping *en échelon* fault segments along the Thamalakane Fault. Illumination is from the NE. Refer to Figure 2a for the area location. (b) Structural interpretation map of Figure 3a. (c) Ternary magnetic anomaly map showing continuous hard linked segments along the Kunyere and the Thamalakane faults. The area shown in Figure 3a is enclosed in a black box. (d) Structural interpretation map of Figure 3c. Fault labels are same as in Figure 2a.

3.2 Aeromagnetic Data

The aeromagnetic data were acquired in 1996 under the direction of the Geological Survey of Botswana. The flight elevation was 80 m along north-south lines with spacing of 250 m and tie lines were east-west (spaced 1.25 km apart). The international geomagnetic reference field was removed and data were gridded (i.e., with a grid cell size of 62.5 m) using minimum curvature technique [*Briggs*, 1974; *Swain*, 1976]. Minimum curvature gridding is accomplished by fitting a smoothest possible surface to data values. First and second vertical derivative filters were applied to the total field magnetic data in order to enhance shallow seated features of the rift and the basement. Ternary maps were prepared in order to enhance basement structural features such as dikes, faults, fractures, and folds. A ternary diagram is a map made by combining color attributes of three separate datasets; in this study optimum enhancement of basement structures was obtained by plotting the total magnetic field, vertical derivative, and analytical signal data into one color map (Fig. 3c, 4c, 5c, and 6c). Analytical signal is the square root of the sum of squares of derivatives in three orthogonal directions as shown in the equation below

$$Analytical\ signal = \sqrt{\left(\frac{\partial^2 T}{\partial x^2} + \frac{\partial^2 T}{\partial y^2} + \frac{\partial^2 T}{\partial z^2}\right)} \qquad (1)$$

Analytical signal is useful in locating the sources of magnetic bodies [Geosoft, 2006]. Structural interpretation maps were made from the ternary maps by tracing lineaments and defining boundaries between domains of distinctly different magnetic character (Fig. 3d, 4d, 5d, and 6d). Depths to the top of magnetic sources calculated from 3-D Euler

deconvolution presented in *Kinabo et al.,* [2006] were used to determine the vertical displacements along the faults. The 3-D Euler deconvolution technique uses the derivative of the signal in three dimensions (xyz) to estimate depth from an arbitrary surface to the top of a representative structure. The technique uses the Euler homogeneity equation which can be written in the form below

$$(x - x_0)\frac{\partial T}{\partial x} + (y - y_0)\frac{\partial T}{\partial y} + (z - z_0)\frac{\partial t}{\partial z} = N(B - T) \qquad (2)$$

Where (x_0, y_0, z_0) is the position of a magnetic source whose total field T is detected at (x, y, z) (Thompson, 1982). The total field has a regional value of B and N is the structural index.

Parameters for the depth estimates included a structural index of 1 for dikes, which were used as displacement markers because of their pervasiveness in the area and their crosscutting relationship with the rift faults. Depth solutions with depth tolerance of greater than 5% were discarded. Vertical throws across faults were estimated by taking the difference in depth between two segments of the dike displaced by faults (Fig. 7).
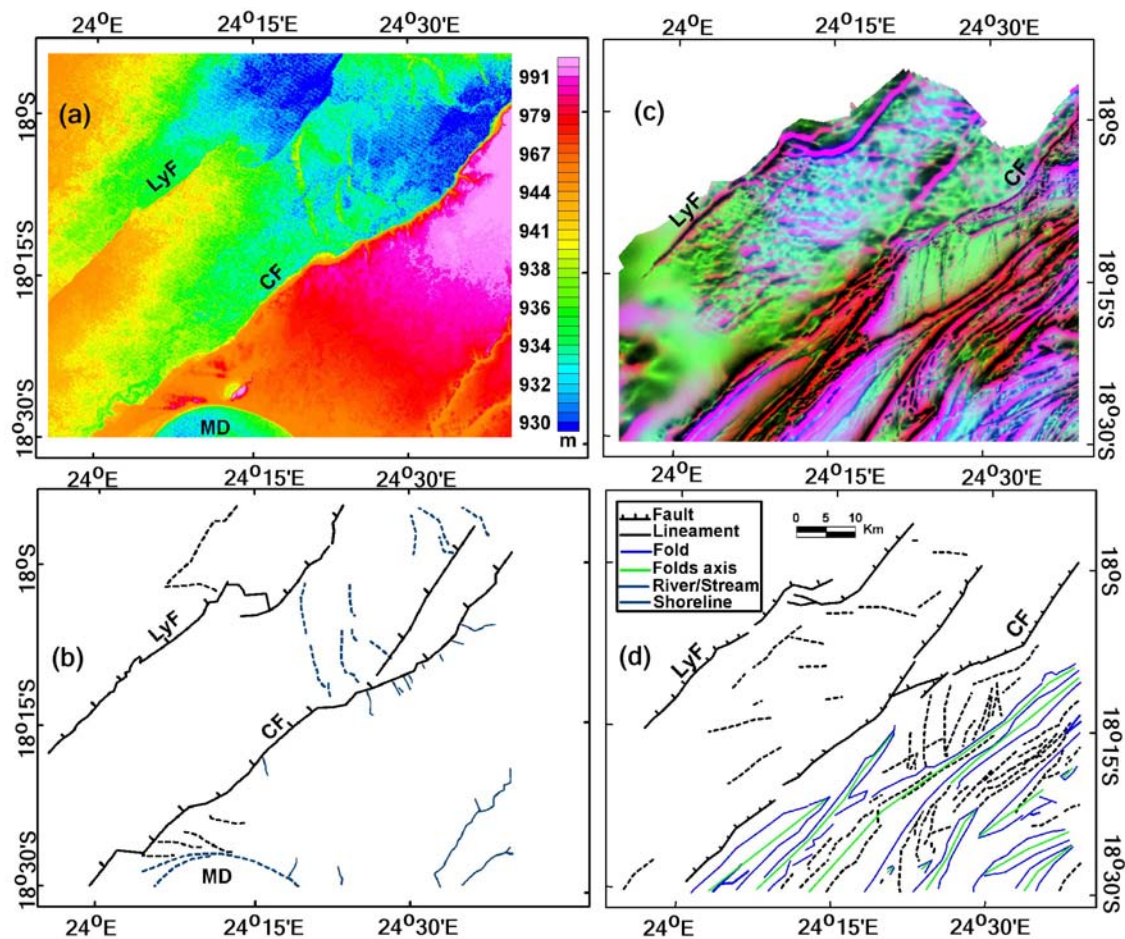
Figure 4: (a) SRTM DEM map showing hard linkage along the Linyanti and Chobe faults. Refer to Figure 2a for the area location. (b) Structural interpretation map of Figure 4a. (c) Ternary magnetic anomaly map of the same area. Note the folds in the basement as revealed by a ternary map. (d) Structural interpretation map of the Figure 4c. Labels are the same as in Figure 2a.

3.3 Interpretation and Mapping of Lineaments

Suspected fault scarps were identified on the DEM by the presence of abrupt changes in elevation along dominantly linear to slightly curving topographic features.

The slope convexities of suspected fault scarps were then analyzed by extracting topographic profiles across the suspected fault scarps from the DEM data. Slope convexity is a measure of gentleness of a slope. In this analysis fault related slopes are assigned zero values, depositional slopes +1 values and the erosion slopes -1 values. The results of this analysis were used to confirm that the topographic features are fault related and not erosion or deposition structures. In addition, the known reported locations for faults in the ORZ [e.g., *Modisi et al.,* 2000; *Kinabo et al.,* 2007] were used to confirm the presence of faults as interpreted from the DEM data. Other pronounced lineaments on the DEM, presumably corresponding to fractures, dikes, and in other locations, stream channels, were noted and mapped. Rose diagrams were constructed using the azimuth of these lineaments to facilitate evaluation of spatial correlations and interpretation of these features.

In the high resolution aeromagnetic data, faults were identified by the presence of abrupt changes in the magnetic character or fabric, the magnitude of the vertical derivative, magnetic intensity, and/or by truncation of prominent magnetic anomalies known to be related to the ESE-WNW Karroo dike swarm [*Modisi et al.,* 2000] along dominantly linear to slightly curving lineaments that typically have very pronounced analytical signals. Other pronounced lineaments in the aeromagnetic data set, presumably corresponding to dikes, basement fractures, lithologic layering, and the trace of fold axes, were noted and mapped. Rose diagrams were constructed using the azimuth of these lineaments. The location of suspected fault boundaries, and other mapped lineaments in the aeromagnetic map were then compared with fault scarps and lineaments identified on the DEM to evaluate their degree of spatial correlation.
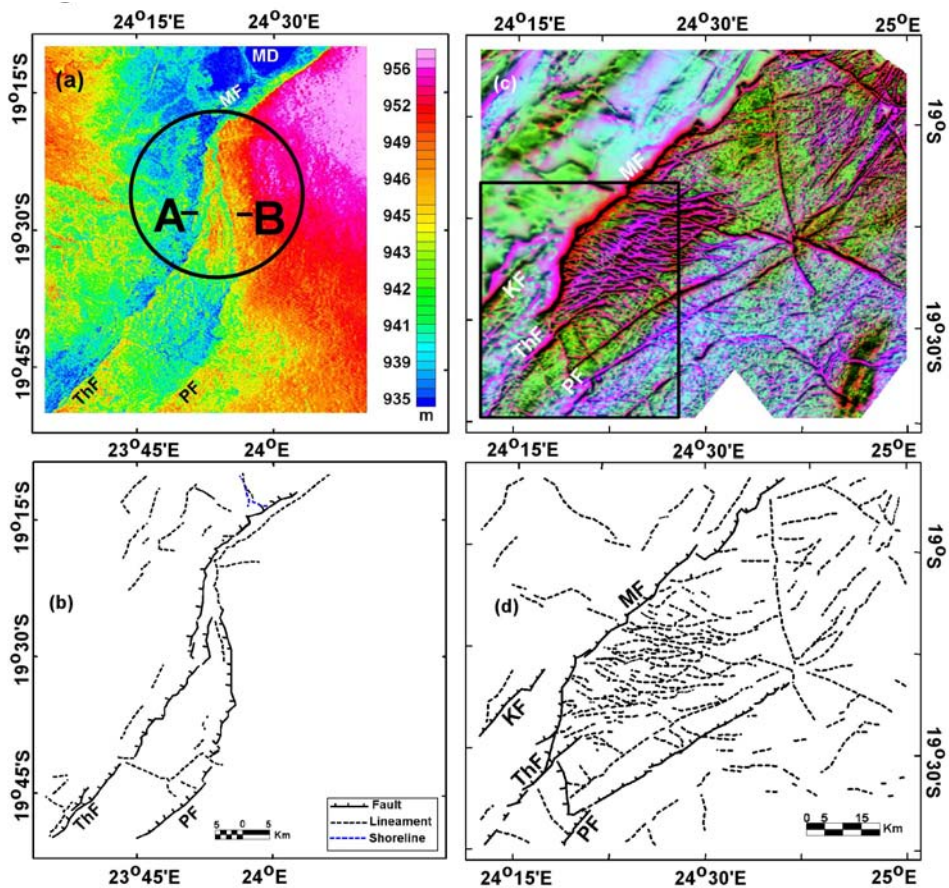
Figure 5: (a) SRTM DEM image showing linkage of the Thamalakane and Phuti faults to the Mababe fault. Refer to Figure 2a for the area location. The black circle encloses A (channel A) and B (channel B) which occupy fractures linking the Thamalakane Fault to the Mababe Fault and the Phuti Fault to the Mababe Fault respectively. (b) Structural interpretation map of Figure 5a. (c) Ternary magnetic anomaly map showing hard linkage along the Mababe Fault. The black box shows the area shown on Figure 5a. (d) Structural interpretation map of Figure 5c. Labels are the same as in Figure 2a.

4. Results

Structural maps based upon topographic lineaments in cover rocks and sediments exposed at the surface as depicted on the DEM data and magnetic lineaments in the basement rocks buried beneath this sedimentary cover as depicted in the aeromagnetic are shown in Figures 2-6 for selected regions of the ORZ. The ORZ is defined by eleven recognized major fault systems; they are the Chobe, Linyanti, Mababe, Phuti, Nare, Thamalakane, Tsau, Gumare, Lecha, and Kunyere Fault, and Sekaka Shear Zone (Fig. 2). The physical characteristics of the faults (e.g., total lengths, throw, scarp height, linkage style) as independently determined from the DEM and from the aeromagnetic maps are summarized in Table 1. Our observations are as follows:

4.1 Fault Recognition

Major NE-SW trending topographic lineaments in the DEM data (Fig. 2-6) are interpreted as fault scarps based upon topographic profiles, slope convexity studies, and correspondence with the locations of previously mapped faults [e.g., *Modisi et al.,* 2000; *Kinabo et al.,* 2007]. The orientation and position of the traces of these faults scarps corresponds closely with lineaments in the aeromagnetic data sets which were independently interpreted as the traces of faults crosscutting the basement terranes (Fig. 2-6). Additionally, the orientation of lineaments in the DEM (topographic scarps and stream channel segments) for the two regions (see Fig. 5 & 6) indicate that the strike of fractures and faults in the basement (aeromagnetic map) and the topographic features at the surface are ENE-WSW and ESE-WNW (Fig. 8). It is striking that locally abrupt changes in the drainage pattern of the river channel define segments whose orientations

also closely coincide with the orientations of fractures and faults (Fig. 8). By combining the results of analysis of these two datasets, a *three dimensional view* of rift-related faults can be constructed to characterize the form of the faults that displaced basement structures as they propagated upwards, eventually rupturing the free-surface.

4.2 Fault Separation (throw)

The throw on individual faults as measured by the height of the fault scarp on the DEM and the difference in the depth to the surface of the basement on the aeromagnetic maps reveals three distinct classes of faults within the ORZ (Table 1). The first class of faults are those in which the throw and fault scarp height are approximately equivalent, or "in balance". The GF is the only example of this fault class, and we suggest that this feature identifies it as being one of the youngest faults associated with the rift, which is consistent with the sharp truncation of sand dunes along this fault scarp (Fig. 2). All other faults exhibit a significant imbalance in the throw as measured from the height of the fault scarps and the depth to the basement surface.

The second class of faults is comprised of those that exhibit significant throw on the basement surface but no topographic expression (Fig. 3). Examples of these faults include the Lecha and Tsau Faults. The Lecha Fault is 200 km long with vertical throws of 56-163 m and the Tsau Fault is 100 km in length and has a vertical throw of 43-130 m. These faults occur towards the interior of the rift and appear to be inactive and buried by sediments. We suggest that these faults are among the earliest faults associated with initiation of rifting or that they were reactivated but lacked sufficient energy to rupture the surface (i.e., blind normal faults).

Table 1: Physical characteristics of selected faults of the Okavango Rift Zone. Vertical displacements values were estimated from 3-D Euler Deconvolution calculations (note 3-D Euler Deconvolution was used to calculate the depth to the top of magnetic bodies), scarp heights were obtained from profiles extracted from DEM data. Modified from *Kinabo et al.* [2007].

	Topographic Characteristics			Basement Characteristics	
Fault Name	Digital Elevation Model (DEM) Fault Length (km)	Scarp Height (m)	Convexity	Aeromagnetic Maps Fault Length (km)	Fault Throw (m)
CF	~260	33-44	-0.05-0.02	~150	ND
GF	~168	~20	-0.02-0.02	~180	~17
KF	~172	~6	-0.02-0.02	~325	232-334
LF	NTE	NTE	NTE	~200	56-163
LyF	~150	~8	-0.03-0.02	~75	ND
MF	~96	12-18	-0.03-0.01	~100	~521
NF	NTE	NTE	NTE	~25	~71
PF	~38	~2	0.01-0.02	~65	~18
ThF	~154	~18	-0.03-0.04	~100	~80
TF	NTE	NTE	NTE	~225	43-130

§ NTE No Topographic Scarp

€ ND   Not Determined
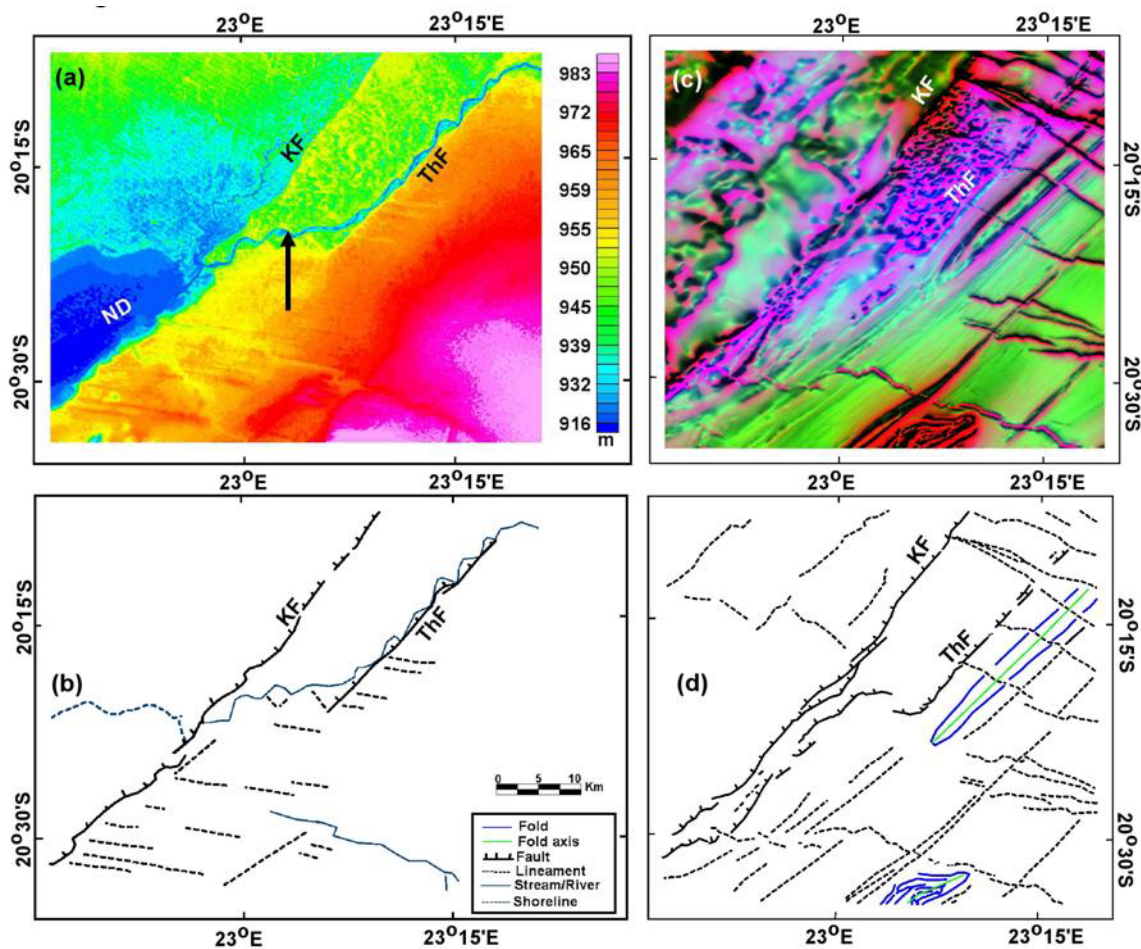
Figure 6: (a) SRTM DEM map showing a connecting fault (shown by an arrow) linking the Kunyere and Thamalakane faults. Refer to Figure 2a for the area location. (b) Structural interpretation map of Figure 6a. (c) Ternary magnetic image of the same area as Figure 6a. (d) Structural interpretation map of Figure 6c. Labels are the same as in Figure 2a.

The third class of faults exhibit large throws on the basement but relatively subdued fault scarps. For example, the Kunyere Fault has a throw on the basement of 232-334 m yet the fault scarp is only 6 m high. The Chobe Fault, Mababe Fault, and

Thamalakane Fault all exhibit fault scarps above 10 m in height and 10s to 100s of meters of throw where determined. We suggest that low relief across the Kunyere Fault scarp reflects waning activity along this fault. Similarly, those faults with significant relief (>10 m) across their scarps indicate these faults have become the locus for recent fault activity.

Faults in which the scarp height and throw are out of balance and still exhibit fault scarps require multiple distinct periods of displacement accompanied by accumulation of sediment on the down thrown block and/or erosion of the fault scarp. Additional evidence for multiple displacement events can be observed from the topographic profiles across several of the fault scarps (Fig. 9). The presence of "knick points" in the Mababe and Thamalakane Fault scarps subdivides the profiles into multiple upper and lower scarps (Fig 9b & c). The topographic slope on the scarp above the knick point has been modified by erosion. The topographic slope on the scarp below the knick point does not appear to have been significantly modified by erosion (Fig. 9c). We interpret the topographic bench developed at the height of the knick point to reflect retreat of the fault scarp as a result of erosion during the hiatus between episodes of faulting. This requires that the multiple episodes of faulting to have been sufficiently recent and spaced closely enough that erosion has not removed the topographic evidence of the older displacement. Alternatively, the benches may also reflect changes in local base level (Fig. 9b), which is consistent with the presence of well marked former shorelines of lake Mababe (Fig. 2). The extent to which changes in local base level is in turn influenced by faulting remains to be constrained.
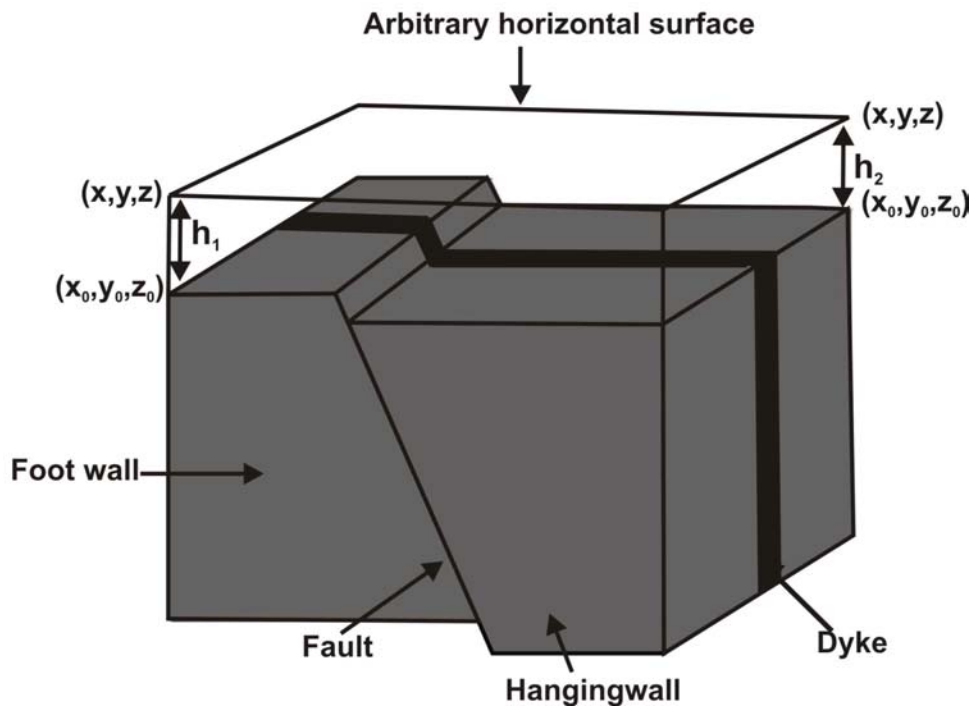
Figure 7: Schematic diagram illustrating the use of dikes as markers for estimating faults vertical throw using 3-D Euler deconvolution technique. Fault throw across the fault shown on the diagram is given by h_2-h_1. Note that the sediments have a near zero magnetic susceptibility and therefore they are not a factor in estimation of the fault throw.

4.3 Fault Separation (heave)

Lateral offset of individual dikes of the Karroo Dike Swarm potentially can provide a sense of the relative magnitude of the heave along these faults, especially if the dikes have near vertical dips. In general, the traces of the dikes show little horizontal offset, indicating that the majority of the movement along the faults is dip-slip in nature [*Modisi et al.*, 2000]. Locally, faults can exhibit evidence for a strike-slip component. For example, along the Thamalakane Fault the magnetic expression of the Karroo Dikes display a right lateral separation (≤ 1 km; Fig. 3c). However, to the south similar

lineaments display a left-lateral sense of displacement along an unnamed fault in the basement (Fig. 6c). It is unknown whether this reflects a true-slip component or is simply apparent slip due to locally some dikes having less than vertical.dips.

4.4 Fault Segmentation

On the DEM fault systems commonly are comprised of several individual fault segments readily recognizable as discrete topographic scarps. Measured at the surface, segments within the fault systems are 3-25 km in length. Within a particular fault zone, the style of fault linkage between the different fault segments can be interpreted from the topographic patterns of the fault scarp lineaments on the DEM. Styles of fault linkages present in the ORZ include: (i) under-lapping (discrete or non overlapping) fault segments as in the case of the ~3-8 km long segments along the Kunyere Fault (Fig. 3a & b) where the spacing between the fault segments is in the range of ~2.5-3 km, (ii) overlapping of right stepping *en échelon* fault segments that are ~3-15 km in length observed along the Thamalakane Fault (Fig. 3a & b), (iii) hooking or touching of segment tips, exemplified by the Linyanti Fault (Fig. 4a & b), and (iv) along-strike bending of fault segments (fused segments) as observed along the Mababe Fault (Fig. 5a & b) and Gumare Fault (data not shown).

The degree and style of fault segmentation of individual fault zones characterized from the topographic expression of the fault scarps on the DEM can differ from that determined from the expression of the same fault on the aeromagnetic map. For example, the Kunyere Fault is composed of four segments that are 3-8 km long on the DEM whereas on the aeromagnetic map it is a continuous fault composed of possibly two segments that are 20 and 50 km in length (Fig. 3). The DEM expression of the

Thamalakane Fault (fig. 3a &b) is characterized by *en échelon* right stepping segments that are 3-15 km long while the aeromagnetic expression of the same fault is characterized by fewer relatively longer (~20-30 km in length) fault segments (Fig. 3c & d). In contrast, the Chobe Fault Zone shows a nearly continuous fault scarp along its entire length in the DEM and appears to consist of several distinct anastomosing segments in the aeromagnetic map (Fig. 4).

4.5 Fault Linkages

Linkage of fault segments within the same fault zone can be observed on both the DEM and aeromagnetic maps. The Linyanti Fault Zone preserves evidence for a hard linkage between two fault segments by hooking. In both the DEM and the aeromagnetic map the trace of these faults bend toward each other to overlap without merging (Fig. 4). To the southeast of the Linyanti Fault, the topographic trace of the Chobe Fault also displays the relicts of a system of right-stepping *en échelon* segments that have essentially merged into a continuous fault scarp. In the aeromagnetic map the linkage between two overlapping fault segments along a right-handed step over forming the current Chobe Fault is clearly marked by a zone of tightly spaced anastomozing faults and fractures. To the northwest of this hard linkage, the trace of the former fault tip is well marked as a magnetic high but with little displacement between the two sides of the fault.

Evidence for linkage of major fault zones which are sub-parallel to the rift can also be seen on the DEM and aeromagnetic maps. For example, different styles of fault linkages between the Kunyere Fault and the Thamalakane Fault can be observed along strike between these two fault systems (Fig. 2). Beginning at the southern end of the

ORZ, within the Ngami Depression the linkage is accentuated on the DEM by a bend and then abrupt deflections in the orientation of the main channel of the Thamalakane River, which flows along the Thamalakane Fault scarp (Fig. 6a & b). Here the main Thamalakane Fault scarp peters out into a zone of less well pronounced, but abundant ~east-west lineaments. On the aeromagnetic map the trace and throw along the Thamalakane Fault dissipates along strike to the south and the Kunyere Fault zone is characterized by multiple fault segments, one of which hooks eastward towards the Thamalakane Fault (Fig. 6c &d). We interpret this to represent a soft linkage along a lateral ramp between these two normal faults (e.g., see Cartwright et al., 1995). Along strike to the north these two fault zone remain distinct (Fig. 3). On the DEM the more subtle trace of the Kunyere Fault dissipate along the strike to the north whereas the Thamalakane Fault is more pronounced and well segmented (see also Fig. 5a &b). On the aeromagnetic map the trace and displacement along the Kunyere Fault also dissipates towards the north which represent the tip of this fault. Additionally, the throw on the basement is significantly larger than that observed for the fault scarp (Table 1). In the basement, the trace of the Thamalakane Fault exhibits fewer segments than on the DEM. To the north the DEM for this area shows the Thamalakane and Phuti Faults both converging into the Mababe Fault as each fault system hooks towards the other (Fig. 5a & b). However, the convergence of these fault zones by hooking is not obvious on the aeromagnetic anomaly maps even thought it appears to be present (Fig. 5c & d). Instead, the trace of the Thamalakane Fault zone overlaps with that of the Mababe Fault before ending in a diffuse zone of abundant lineaments that we interpret as fractures and minor faults (Fig. 5). The Phuti Fault also appears to continue to the north and an additional

fault, not recognized in the DEM, parallels the trace of this fault. The soft linkage of these faults zone is occurring across this diffused strain zone.
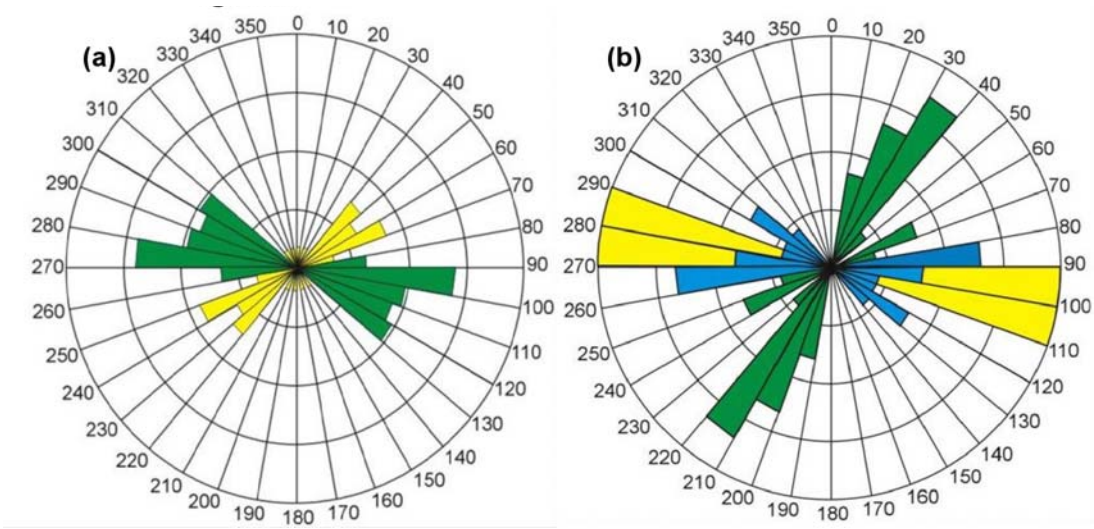
Figure 8: Rose diagram showing the orientation of faults, fractures and streams in the ORZ. (a) azimuth of fractures from the area shown on Figure 5c. Green = ESE-WNW trending fractures and Yellow = ENE-WSW trending fractures. (b) Azimuth of fractures, faults and stream in the area shown on Figure 6a. Green = fault segments, Blue = streams, Yellow = fractures.

5. Discussion

5.1 Fault Characteristics

All the faults mapped on the aeromagnetic maps except Lecha and Tsau have scarps associated with their surface expressions (Fig 3; Table 1). The lack of surface expression for these basement faults may indicate 1) inactivity during the extensional tectonic regime associated with the ORZ, 2) that these basement faults were reactivated, but are now concealed by rapid sedimentation associated with Okavango alluvial fan deposits, and 3) they were reactivated but lacked sufficient energy to rupture the surface (i.e., blind normal faults). The scarp heights are significantly smaller than the fault throw values calculated from the 3-D Euler deconvolution solutions (Table 1). The discrepancy is as much as 500 m along the Mababe Fault. This suggests either higher sedimentation rates from the Okavango River compared to the vertical movement along the faults leading to partial burial or moderate sedimentation rates against little to no vertical recurrent movement along the faults. Recent seismic events along the major rift faults support the higher sedimentation rates scenario [*Scholz et al.*, 1976].

Within the ORZ, major fault zones and their segments have orientations that parallel the structural fabric of the basement. This strength anisotropy in the basement greatly influenced the location and orientation for brittle failure. The low displacement to length scaling relations observed for these faults may in part reflect a reduction in the stress required to produce failure and laterally propagate faults along these pre-existing planes of weakness. In addition, comparison of the throw on the basement surface with the throw on the topographic fault scarp demonstrates many of the faults have extended

histories. Most of the faults suggest evidence for multiple episodes of faulting with concomitant sedimentation along the down thrown block and erosion of the fault scarps. Thus, older faults that have established long fault traces as a result of multiple episodes of faulting and through linking of fault segments (see below) may exhibit topographic scarps with less relief as a result of: 1) the height of the topographic fault scarp reflects only the most recent displacement event that ruptured the surface, 2) since the last displacement, the height of the fault scarp has been reduced by sedimentation, and/or 3) the height of the fault scarp has been reduced by erosion.

5.2 Fault Growth and Propagation

Combining the results from the two data sets allows us to better evaluate the three dimensional geometry of the fault planes, and therefore the growth of faults through fault linkages based upon the patterns of fault scarps in the DEM and fault traces in the aeromagnetic maps. For example, the traces of the Thamalakane, Kunyere, and Phuti faults are segmented on the DEM map but are continuous on the aeromagnetic map (Fig. 3). The faults initiate at depth within the basement as long continuous faults. As the leading edge of the propagating fault plane approaches the topographic surface twists, similar to those which form along the margins of joints, develop and rupture the surface (Fig. 10). These twists will appear as *en échelon* fault segments on the DEM and could be erroneously interpreted as discrete fault planes related by soft linkage all the way down to the basement. Similarly, continuous fault scarps on the DEM can overlay segmented fault traces in the basement (e.g., the Chobe Fault; Fig. 4). This continuous nature of the topographic scarp may be the result of a combination of fault scarps connected by erosion scarps.
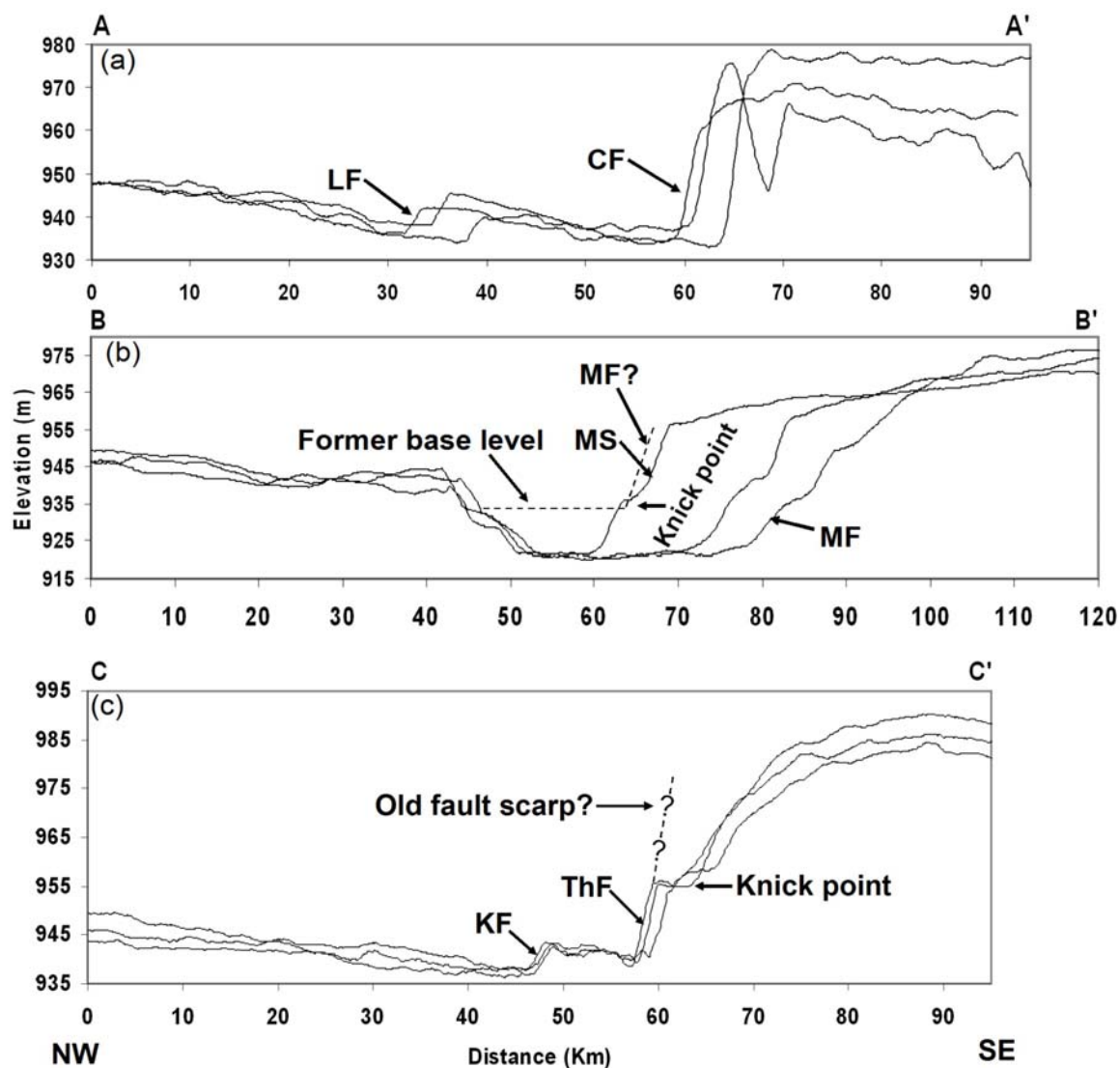
Figure 9: Profiles showing scarps in the ORZ. (a) profiles A-A' along the Linyanti Fault (8 m) and the Chobe Fault (33-44 m), profile are ~10 km apart. (b) Profile C-C' along the Mababe Depression, Mababe Scarp (12-18 m); profiles are > 13 km apart. (c) Profiles B-B' along the Kunyere Fault (6 m) and the Thamalakane Fault (18 m), profiles are > 4 km apart. See Figure 2a for the location of the profiles. The annotation on the bottom of profile C-C' and to the left of profile B-B' apply to all profiles. MS = Mababe topographic Scarp, other labels are the same as in Figure 2.
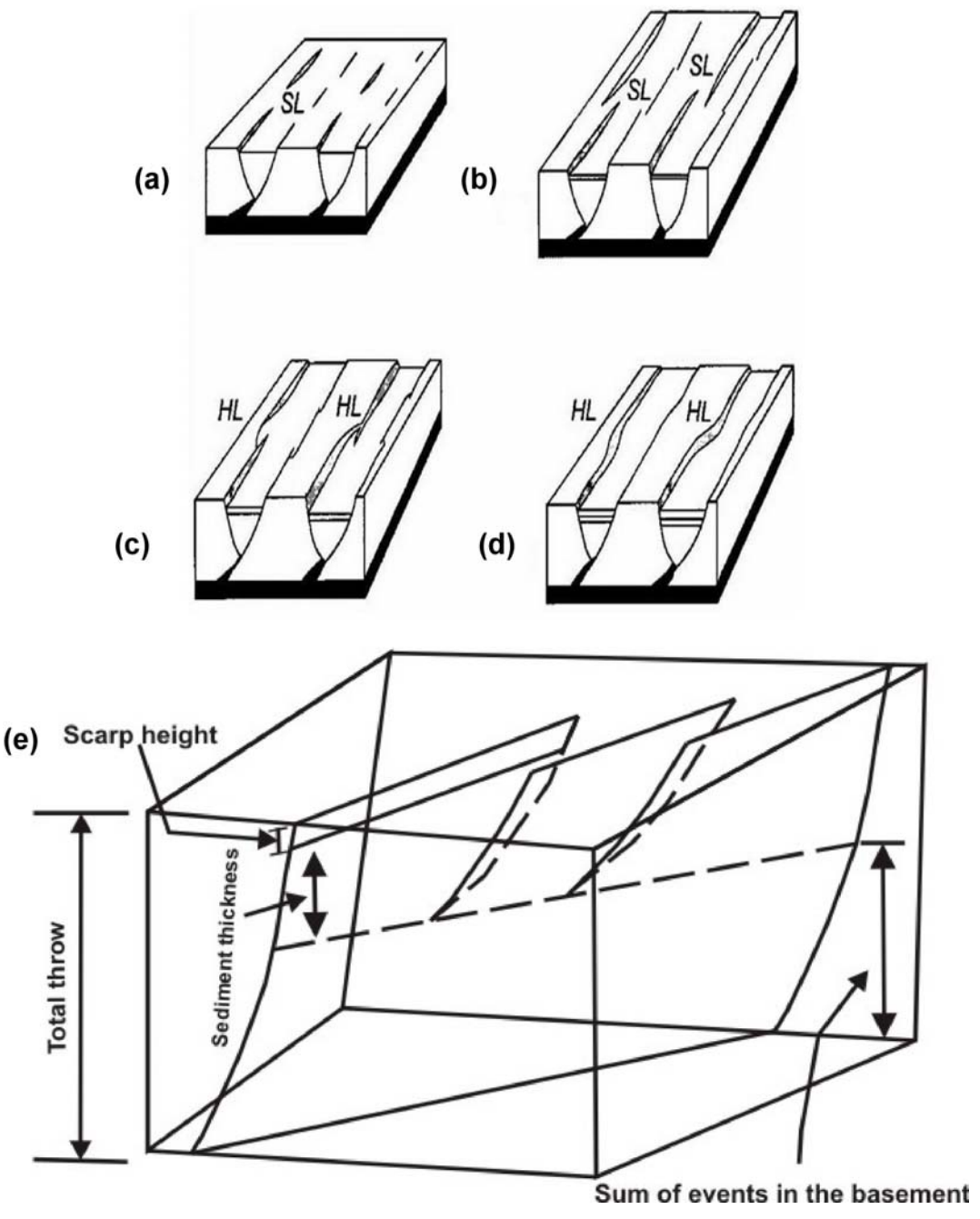
Figure 10: (a) Model showing fault growth and linkage in a progressively increasing stress extensional environment. Modified from Le Calvez and Vanderville, 2002. (b) En echelon segments at the surface may be twists connected to the same fault plane at depth as exemplified by portions of the Kunyere Fault and Thamalakane Fault in Figure 3.

With these cautions in mind, the results of the combined aeromagnetic and DEM investigations are consistent with a model for fault evolution beginning with short discrete fault segments (3-25 km long) which propagate and eventually merge to form long continuous fault segments (~25-325 km long). *Trudgill and Cartwright*, [1994] proposed a 2-D evolutionary model in progressively increasing stress environment in which faults grow from soft to hard linkage of small originally isolated fault segments. Soft-linkages are characterized initially by under lapping segments, which with increased stress continue to propagate and eventually overlap and form relay ramps. Further increase of stress leads to the development of hard linkages, which is marked by development of connecting faults on the relay ramp to complete fusion of originally isolated segments (Fig 10). Using this model we interpret that faults in ORZ are at different temporal stages of fault evolution.

The results of this study extend the initial findings of *Kinabo et al.,* [2007] and help clarify the development of rift faults based on the observations from both the basement and the surface geomorphology by coupling aeromagnetic with DEM data. We suggest two hierarchical orders of linkage patterns in ORZ: (1) first order linkage where two or more major sub parallel rift faults are linked by connecting faults (Fig. 5 & 6), and (2) second order linkage that is achieved through soft to hard linkage of small *en échelon* segments along the axis of a single fault (Fig. 3 & 4). For example, segments within portions of the Thamalakane Fault and the Linyanti Fault systems exhibit patterns consistent with the development of soft linkages (Fig. 3 & 4). The Chobe Fault shows evidence of a hard linkage forming between two *en échelon* right-stepping segments leading to abandonment of a portion of the former fault tip (Fig. 4). The Kunyere, and

Mababe Faults exhibit more continuous faults traces (i.e., fewer segments) indicating a more advanced stage of linkage (Fig. 3, 4, 5, & 6). The larger throws on the basement for the Kunyere and Mababe faults (Table 1) are consistent with an advanced stage of fault evolution.

5.3 Development of Border Faults

Border, master or -basin faults are defined as faults that bound the rift basins [*Peacock and Sanderson,* 2000 and references therein]. The characteristics of border faults include larger displacement and length when compared to other faults within the same rift. A particular rift zone can have one or multiple border faults depending on the number of basins within the rift. For example, the Rio Grande Rift has 4 border faults one for each of the four basins that make up the rift, Malawi Rift has three border faults for its three basins [*Chorowicz,* 2005; *Chapin and Cather,* 1994]. Following the same definition *Kinabo et al.,* [2007] reported that the border fault in the ORZ is still in a juvenile stage. This interpretation was based solely on the vertical displacements along faults obtained from 3-D Euler deconvolution solutions and length of the faults observed on the aeromagnetic data.

Within the ORZ, border faults are still developing through the formation of soft and subsequently hard linkage of several rift-related faults. In addition to linkage of segments along the axes within individual fault zones, linkages are also developing between the major rift faults. The Kunyere Fault is transferring strain to the Thamalakane Fault along a soft linkage defined by a lateral ramp between overlapping segments of these two fault zones (Fig. 3) and to the south along a soft linkage characterized by hooking of the fault tips and diffusion of the strain along closely spaced parallel fault

segments and a diffuse set of ~east-west fractures oriented approximately 75° clockwise from the strike of the main fault zones (Fig. 6). The patterns for subsidiary faults and fractures to the main fault traces are consistent with those of Riedel shears associated with right-lateral strike-slip (Fig. 8). Thus, the transfer of strain from one fault to other may be influenced by pre-existing fractures in the basement as well as a component of right-lateral strike slip, which for a system of right-stepping faults would lead to extension. To the north the Thamalakane Fault partially overlaps the Mababe Fault creating what was initially a soft-linkage by transferring strain over a diffuse domain characterized by abundant minor faults and fractures. This soft-linkage evolved to a hard linkage as connecting faults between the Thamalakane and Mababe Faults, visible on both the DEM and aeromagnetic map, were established (Fig 5). Here the two faults are left-stepping, which would create a local zone of compression within the area of overlap between the faults if there is indeed a component of right-lateral strike slip to the displacement. This may explain why the intervening zone is intensely deformed by brittle faults and fractures (Fig. 5c). It should be noted that lateral offset of linear markers (e.g., Karroo Dikes) along the fault traces suggest both left lateral and right lateral separation along rift related faults. Additionally, the overall form of the main faults bordering the major deposition centers is left stepping. Thus the extent to which a strike slip component is significant in the development of the ORZ remains unclear.

Previously, the Kunyere Fault system has been considered the border fault for the ORZ [*Modisi et al.*, 2000]. This interpretation was based on the substantial, nearly continuous length of the fault trace and the significant amount of throw observed on the basement surface (Table 1). However, our analysis of fault linkages suggests that a new

master border fault system is in the process of emerging. This master border fault is be created as a result of linkages between portions of the Kunyere Fault system and the Thamalakane Fault system in the south, and the Thamalakane Fault and Phuti Fault systems to the Mababe Fault system along strike to the north. This interpretation is supported by the subdued topographic scarp above the Kunyere Fault which suggests waning displacement along this fault trace (Fig. 3). In contrast to the subdued scarp height along the Kunyere, significant topographic fault scarps are present along the Thamalakane and Mababe Faults consistent with recent activity and displacement along these faults. The linking of these large fault systems into a master border fault serves to increase the overall length of the rift by connecting the different deposition centers (Fig. 2). The older and significantly less active faults occur towards the center of the rift, whereas the younger and more active faults now occur on the margins of the rift. Thus, the rift also widens as it matures by retiring older border faults, such as portions of the Kunyere, through transfer of strain to a now much larger faults systems (in length) along the margins of the rift – a process that may be called *"Fault Piracy"*.

5.4 Neotectonics and Fluvial Systems

The main fault zones, the linkages between these zones, and pre-existing basement fabrics appear to be exerting a profound influence on the drainage patterns of the fluvial systems in the ORZ. Linkages between major fault zones are commonly areas of intense fracturing that have been influenced by the orientation of basement fabrics and are exploited by stream/river erosion. For example, in the south the Thamalakane River flows along the Thamalakane Fault and exhibits abrupt deflections (rather than smooth meanders) in the orientation of its course (as seen on DEM) that define a pattern of right

stepping *en échelon* river channel segments (Fig. 6). South of 20°15'S the river flows in an almost east-west direction, cutting through the Kunyere Fault and into Lake Ngami along NE trending right stepping *en échelon* segments. In the north, the interaction of the Thamalakane Fault and the Mababe Fault coincides with a NNE trending stream (channel A; Fig. 5a & b) while the interaction between the Phuti Fault and the Mababe Fault is highlighted by a NNW trending stream channel B (Fig. 5a & b). Fractures orientation on DEM and aeromagnetic maps display pronounced ~ESE-WNW and also SSW-NNE and SSE-NNW trends coinciding with stream channels (Fig. 5, 6 & 8). Similarly, a study by *Wormald et al.*, [2003] found out that pans are also aligned 030°-050° and 130°. The pans develop along the southern side of the ORZ reflecting the general SE tilt of the faults blocks along listric normal faults (Fig. 2 & 9). Hence, it appears that faults and fractures are exerting a profound influence on the location and development of the river/stream channels and pans highlighting the coupling of neotectonic and fluvial activities in the ORZ.

6. Conclusions

The integration of high resolution aeromagnetic with DEM data provides important insights into fault growth and propagation associated with the ORZ. Coupled analysis of SRTM DEM and aeromagnetic data has revealed that (1) the growth of individual rift faults occurs by along axis linkage of small segments; (2) based on the relationship between fault throws and scarp heights, the faults in the ORZ can be categorized into four groups (a) old and active such as the Thamalakane and Mababe faults, (b) young and active, for example the Gumare Fault, (c) faults with no recent activity such as the Lecha and Tsau faults, and (d) faults with waning activity, for example the Kunyere Fault; (3) border fault system is developing by linkage of major sub-parallel rift faults through fault piracy resulting in lengthening and widening of the rift basin; (4) pre-existing basement structures influence the development of the main rift-related faults and the linkages between these faults allowing the rift faults to grow so long (up to > 300 km) without much displacements along them; (5) faults in the ORZ are at different temporal stages of evolution; (6) fluvial morphology is greatly influenced by basement structures suggesting coupling of neo-tectonic and surficial processes in this incipient rift; (7) the spatial distribution of the major rift-related faults and subsidiary fractures indicate the possibility of a right-lateral strike-slip component in addition to the normal slip component as being important to the formation of this rift; and (8) coupling of DEM with aeromagnetic data analysis is a powerful tool for studying rift kinematic processes and can significantly augment field studies, especially in areas with limited basement exposures.

Acknowledgements

References

Anders, M. H., and R. W. Schlische, (1994), Overlapping faults, intrabasin highs and growth of normal faults, *Journal of Geology*, 102, 165-180.

Briggs, I. C., (1974) Machine contouring using minimum curvature, *Geophysics*, 39, 39-48.

Cartwright, J. A., B. D. Trudgill, and C. S. Mansfield, (1995), Fault growth by segment linkage: an explanation for scatter in maximum displacement and trace length data from Canyonlands Graben of SE Utah, *J. Struct. Geol.*, 17, 9, 1319-1326.

Chapin, C. E., and S. M. Cather, (1994), Tectonic setting of the axial basins of the northern and central Rio. *Geological Society of America special paper*, 291, 5-25.

Chen, L., and L. Lee, (1992), Progressive generation of control frameworks for image registration, *Photogrammetric Engineering and Remote Sensing*, 58, 1321-1328.

Chorowicz, J., (2005), The East African rift system. *J. African Earth Sci.*, 43, 379-410.

Cowie, P. A., and C. H. Scholz, (1992). Displacement-length scaling relationships for faults: data synthesis and discussion. *J. Struct. Geol.*, 14, 1149-1156.

Cowie, P. A., (1998a), Normal fault growth in three dimensions in continental and oceanic crust. *Geophysical Monograph*, 106, 325-345.

Cowie, P. A., (1998b), A healing-reloading feedback control on the growth rate of seismogenic faults: *J. Struct. Geol.*, 20, 1075–1087.

Davis, S. J., N. H. Dawers, A. E. McLeod, and J. R Underhill, (2000), The structural and sedimentological evolution of early synrift succession: the Middle Jurassic Tarbert Formation, North Sea. *Basin Research*, 12, 343-365.

Dawers, N. H., and M. H. Anders, (1995), Displacement-length scaling and fault linkage, *J. Struct. Geol.* 17,607-614.

Ebinger, C. J., (1989), Tectonic development of the western branch of the East African Rift System. *Geol. Soc. Am. Bull.*, 101, 885-903.

Grauch, V. J. S., (2001), High-resolution aeromagnetic data, a new tool for mapping intrabasinal faults: Example from the Albuquerque basin, New Mexico. *Geology,* 29, 4, 367–370.

Jackson, C. A., R. B. Gawthorpe, and I. R. Sharp, (2002), Growth and linkage of the East Tanka fault zone, Suez Rift: structural style and synrift stratigraphic response, *J. Geol. Soc. London*, 159,175-187.

Kervyn, F., S. Ayub, R. Kajara, E. Kanza, and B. Temu, (2006), Evidence of recent faulting in the Rukwa rift (West Tanzania) based on radar interferometric DEM, *J. African Earth Sci.*, 44, 151-169.

Kinabo, B. D., E. A. Atekwana, J. P. Hogan, M. P. Modisi, D. D. Wheaton, and A. B. Kampunzu, (2007), Early structural evolution of the Okavango Rift Zone, NW Botswana, *J. African Earth Sci.,* v. 48, p 125-136.

Le Calvez, J. H., Vendeville, B. C., 2002, Physical modeling of normal faults and grabens above relay above salt. Gulf Coast Association of Geological Socities, 52, 599-606.

Le Gall, B., G. Tshoso, F. Jourdan, G. Fèraud, H. Bertrand, J. J. Tiercelin, A. B. Kampunzu, M. P. Modisi, J. Dyment, and M. Maia, (2002), $^{40}Ar/^{39}$ geochronology data from the giant Okavango and related mafic dyke swarms, Karoo igneous province, northern Botswana. EPSL, 202, 595-606.

Macheyeki, A. S., D. Delvaux, F. Kervyn, and E. B. Temu, (2005), Morphotectonics of the Kanda fault system in the Ufipa plateau, *in Extended Abstracts on the International conference on the East African Rift System*, *Mbeya, Tanzania,* pp 53-57, edited by Atekwana et al., University of Dar es Salaam, Geology and Geography Department*s*.

McClay, K. R., T. Dooley, P. Whitehouse and M. Mills, (2002), 4-D evolution of rift systems: Insights from scaled physical models. *AAPG Bulletin*, 86, 6, 935-959.

Modisi, M. P., E. A. Atekwana, A. B. Kampunzu, and T. H. Ngwisanyi, (2000), Rift Kinematics during the incipient stages of continental extension: Evidence from the nascent Okavango rift basin, northwest Botswana, *Geology*, 28, 939-942.

Morley, C. K., (1999), How successful are analogue models in addressing the influence of pre-existing fabrics on rift structure? *J. Struct. Geol.,* 21, 1267-1274.

Morley, C. K., 2002, Evolution of large normal faults: Evidence from seismic reflection data. *AAPG Bulletin*, 86, 6, 961-978.

Moustafa, A. R., (2002), Controls on the geometry of transfer zones in Suez rift and northwest Red Sea: Implication for the structural geometry of rift systems. *AAPG Bulletin*, 86, 6, 979-1002.

Mulugeta, G., and G. Woldai, (2001), Modeling heterogeneous stretching during episodic or steady rifting of the continental lithosphere, *Geology,* 29, 895-898.

Peacock, D. C. P., and D. J. Sanderson, (1991), Displacements, segment linkage and relay ramps in fault zones, *J. Struct. Geol.*, 13, 721-733.

Ring, U., (1994), The influence of preexisting structure on the evolution of the Cenozoic Malawi rift (East African Rift System), *Tectonics*,13, 313-326.

Rosendahl, B. R., (1987), Architecture of the continental rifts with special reference to East Africa, *Annual Reviews of Earth and Planetary Sciences*, 15, 445-503.

Ringrose, S., P. Huntsman-Mapila, A. B. Kampunzu, W. Downey, S. Coetzee, B. Vink, W. Matheson and C. Vanderpost, (2005), Sedimentological and geochemical evidence for paleo-environmental change in the Makgadikgadi subbasin, in relation to the MOZ rift depression, Botswana. *Paleogeography, Palaeoclimtology, Palaeoecology*, 217, 265-287.

Swain, C. J., 1976, A FOTRAN IV program for interpolating irregularly spaced data using the difference equations for minimum curvature, Computer & Geosciences, 1, 231-240.

Scholz, C. H., T. A. Koczynski., and D. G. Hutchins, (1976). Evidence for incipient rifting in southern Africa. *Royal Astronomical Society Geophysical Journal,* 44, 135-144.

Trudgill, B. D., and J. A. Cartwright, (1994), Relay ramp forms and normal fault linkage Canyonlands National Park, Utah. *Geol. Soc. Am. Bull.*, 106, 1143-1157.

Trudgill, B. and J. R. Underhill, (2002), Introduction to the structure and stratigraphy of rift systems. *AAPG Bulletin*, 86, 6, 931-933.

Walsh, J. J., W. R. Bailey, C. Childs, A. Nicol, and C. G. Bronson, (2003), Formation of segmented normal faults: a 3-D perspective. *J. Struct. Geol.*, 25, 1251-1262.

Withjack, M. O., (1995), Normal faults and their hanging-wall deformation: an experimental study. *AAPG Bulletin*, 79, 1, 1-18.

Wormald, R. J., F. D., Eckardt, J. Vearncombe, and S. Vearncombe, 2003, Spatial distribution of pans in Botswana: the importance of structural control. *South African of Geology*, 106, 287-290.

2. CONCLUSIONS AND RECOMENDATIONS

Investigation of the ORZ in northwestern Botswana using high resolution potential field data (gravity and magnetics), SRTM DEM and field methods offer new insights into the processes operating during the early stages of continental rifting. The results suggest the following major conclusions: (1) Pre-existing basement structures represent a significant strength anisotropy that controlled the development of rift structures including the major rift faults and their linkage; (2) utilization of pre-existing zones of weaknesses (basement fractures, folds) by the young faults allowed faults that are 3-15 km long to link and grow to form major rift faults ~25-325 km long. This also explains the apparent paradox between the faults length (25-325 km) versus throw (17-334 m) for this young rift; (3) the border fault is developing by the linkage of several major rift faults, which occurs through transfer zones by the process of fault piracy; (4) the relationship between fault throws and scarp heights of the faults in the ORZ allows classification of faults into (a) old and active such as the Thamalakane and Mababe faults, (b) young, for example the Gumare Fault, (c) faults with no recent activity such as the Lecha and Tsau faults, and (d) faults with waning activity for example the Kunyere Fault; (5) young and more active rift faults are located on the outer margin of the rift, whereas old and non active faults are in the middle suggesting that the rift grows both in length (by along axis linkage of segments) and width; (6) the geometric shape of the rift basin can be characterized as transitional between a synformal depression and an early half-graben development, consistent with an immature and developing border fault system, and finally (7) the integration of potential field and remote sensing technologies particularly SRTM DEM and aeromagnetic has proven to be a reliable and cost effective

way of studying continental rift in approximately 3-D in areas where field based methods have little success because of subtle topographic relief or thick sediment cover .

Although this study has provided significant insights into the early stages of continental rifting, more work is needed to investigate the following observations: (1) Spatial orientation of fractures and major faults on the Rose diagram and the lateral displacement of dikes on the aeromagnetic data suggest a possible strike slip stress component in addition to the normal stress regime. Field work is necessary in order to confirm this observation and determine the direction of fault motion; (2) Gravity models suggest the presence of shallow seated high density rock mass along the axis of the rift. This gravity anomaly can either be explained as an intrusive mafic body or a horst block. Further investigations can aid in the clarification of the source of this local gravity high; (3) Age dating of the rift faults and the syn-rift sediments will provide critical insights on how much time it takes for rift faults to link together and form a boundary fault; (4) The Lecha and Tsau faults have considerable fault throws but lack topographic scarps. These faults were interpreted to have no recent movements along them. Further geophysical methods particularly those that can detect fault movement within sediments such as seismic and electrical methods are suggested in order to confirm the lack of activity along these faults; and (5) Aeromagnetic data of the Kunyere and Thamalakane faults suggest that the under lapping to overlapping segments observed on the surface along these faults may be connected twists in the basement. Further geophysical imaging (seismic reflection or electrical imaging) is needed to provide data that can bridge the gap between the surface expression of these faults and their basement expression (i.e, how these faults link at depth).

BIBLIOGRAPHY

Ballard, S., Pollack, H. N., and Skinner, N. J., 1987, Terrestrial heat flow in Botswana and Namibia: Journal of Geophysical Research, v. 92, p. 6291-6300.

Bastow, I. D., Stuart, G. W., Kendall, J. M., and Ebinger, C. J., 2005, Upper-mantle seismic structure in a region of incipient continental breakup: northern Ethiopian rift, Geophysical Journal International, v. 162, p. 479-493, doi: 10.1111/j.1365-246X.2005.02666.x

Chapman, D. S., and Pollack, H. N. 1977, Heat flow and heat production in Zambia: Evidence for lithospheric thinning in central Africa, Tectonophysics 41, 79-100.

Chorowicz, J., 2005, The East African rift system. Journal of African Earth Sciences, v. 43, p. 379- 410.

Davis, G. H., and Reynolds, S. J., 1996, Structural geology of rocks and regions: John Wiley and sons, Inc. 2nd edition, 776p.

Ebinger, C. J., 1989, Tectonic development of the western branch of the East African rift system: Geological Society of America Bulletin, v. 101, p. 885-903.

Ebinger, C. J., and Casey, M., 2001, Continental breakup in magmatic provinces: An Ethiopian example. Geology v. 29, 6, p. 527-530.

Ebinger, C. J, 2005, Continental rifting and breakup processes: Insights from East Africa. In Extended abstracts on the International Conference on the East African Rift System-EAR05: Geodynamics, Environment, Resources, and Sustainable Development, Mbeya, Tanzania, edited by Atekwana et al., University of Dar es Salaam, Geology and Geography Departments.

Fairhead, J. D., and Girdler, R. W., 1969, How far does the rift system extend through Africa? Nature, v. 221, p. 1018-1020.

Girdler, R. W., 1975, The great Bouguer anomaly over Africa: eos (Transactions, American Geophysical Union), v. 56, p. 516-519.

Gumbricht, T., Mc Carthy, T. S., and Merry, C. L., 2001, The topography of the Okavango Delta, Botswana, and its tectonic and sedimentological implications. Journal of Structural Geology, v. 104, p. 243-264.

Kampunzu, A. B., Bonhomme, M. G., and Kanika, M., 1998, Geochronology of volcanic rocks and evolution of the Cenozoic Western branch of the East African rift system: Journal of African Earth Sciences, v. 26, p. 441-461.

Keranen, K., and Klemperer, S. L., the EAGLE Working Group., 2004. 3D seismic imaging of protoridge axis in the Main Ethiopian Rift. Geology, v. 32, 11, p. 949-952.

Kinabo, B. D., Atekwana, E. A., Hogan, J. P., Modisi, M. P., Wheaton, D. D., and Kampunzu, A. B., 2007, Early structural evolution of the Okavango Rift Zone, NW Botswana, Journal of. African Earth Science, v. 48, p. 125-136.

Kinabo, B. D., Hogan, J. P., Atekwana, E. A., and Modisi, M. P, Fault growth and propagation during incipient continental rifting: Insights from a combined aeromagnetic and SRTM DEM investigation of the Okavango rift zone, NW Botswana. Tectonics (*in review*).

Mackenzie, G. D., Thybo, H., and Maguire, P. K. H., 2005, Crustal velocity structure across the Main Ethiopian Rift: results from two-dimensional wide-angle seismic modelling, Geophysical Journal International, v. 162, p. 994-1006, doi: 10.1111/j.1365-246X.2005.02710.x.

Maguire, P., and the EAGLE Controlled Source Team, 2003, EAGLE - The Controlled Source Experiment, Geophysical Research Abstracts, v. 5, p. 01264.

Modisi, M. P., Atekwana, E. A., Kampunzu, A. B., and Ngwisanyi, T. H., 2000, Rift Kinematics during the incipient stages of continental extension: Evidence from the nascent Okavango rift basin, northwest Botswana: Geology, v. 28, p. 939-942.

Morley, C. K., Ngenoh, D. K., and Ego, J. K., 1999, Introduction to the East African Rift System, *in* C.K. Morley ed., Geoscience of Rift Systems – Evolution of East Africa: AAPG Studies in Geology, v. 44, p. 1-18.

Morley, C. K., 2002. Evolution of large normal faults: Evidence from seismic reflection data. American Association of Petroleum Geologist Bulletin, v. 6, p. 961-978.

Reeves, C. V., 1972, Rifting in the Kalahari? Nature, v. 237, p. 95-96.

Rosendahl, B. R., 1987, Architecture of the continental rifts with special reference to East Africa. Annual Reviews of Earth and Planetary Sciences, 15, 445-503.

Sebagenzi, M. N., Vasseur, G., and Louis, P., 1993, First heat flow density determinations from southeastern Zaire (central Africa). Journal of African Earth Sciences, v. 16, p. 413-423.

Sebagenzi M. N., and Kaputo K., 2002, Geophysical evidences of continental break up in the southeast of the Democratic Republic of Congo and Zambia (Central Africa). In: S.A.P.L. Cloetingh and Z. Ben-Avraham (Eds.), From continental extension to collision: Africa-Europe interaction, the Dead Sea and analogue natural laboratories. EGU European Geosciences Union, Stephan Mueller Special Publication Series, v. 2, p. 193-206.

VITA

Baraka Damas Kinabo was born on the 9th April, 1975, in Mbeya, southern Tanzania. He started his early education at Majengo Juu Primary School in Mbeya, in 1983. He received a BSc. degree in Geology with honors from the University of Dar es salaam, Tanzania in 2000. He also received a MS. Geophysics degree from Western Michigan University (WMU) in Kalamazoo, MI in 2003 and a PhD in Geology and Geophysics from the University of Missouri-Rolla (UMR) in 2007. He has published one paper in the *Journal of African Earth Sciences* and he has submitted another to *Tectonics,* which is currently under review. He is a member of several professional associations including; Society of Exploration Geophysics (SEG), American Association of Professional Geologists (AAPG), Geological Society of America (GSA), National Association of Black Geologists and Geophysicists (NABGG) and Society of Petroleum Engineers (SPE). He has served as a treasurer and a secretary of the student chapter of SEG at UMR from 2005-2007. His research interests are in Tectonophysics specifically studying the initiation and propagation of continental rifts using potential fields and remote sensing techniques. He also has interests in the application of near surface geophysics to environment and engineering problems. Mr. Kinabo is married to Victoria Joshua Mamkwe and they are expecting a baby in April, 2008.